Interfacial Behaviour in Ferroalloys: The Influence of Sulfur in FeMn and SiMn Systems

SERGEY BUBLIK, SARINA BAO, MERETE TANGSTAD, and KRISTIAN ETIENNE EINARSRUD

The present study has investigated the influence of sulfur content in synthetic FeMn and SiMn from 0 to 1.00 wt pct on interfacial properties between these ferroalloys and slags. The effect of experimental parameters such as temperature and holding time was evaluated. Interfacial interaction between ferroalloys and slags was characterized by interfacial tension and apparent contact angle between metal and slag, measured based on the Young–Laplace equation and an inverse modelling approach developed in OpenFOAM. The results show that sulfur has a significant influence on both interfacial tension and apparent contact angle, decreasing both values and promoting the formation of a metal-slag mixture. Despite the fact that sulfur was added only to the ferroalloys, most of sulfur is distributed into slag after reactions with the metal phase. Increasing the maximum experimental temperature in the sessile drop furnace also resulted in a decrease of both interfacial properties, resulting in higher mass transfer rates and intensive reactions between metal and slag. The effect of holding time demonstrated that after reaching equilibrium in FeMn-slag and SiMn-slag systems (both with and without sulfur), interfacial tension and apparent contact angle remain constant.

I. INTRODUCTION

HIGH-CARBON FeMn and SiMn are produced in submerged arc furnaces (SAF) by carbothermic reduction of manganese ores with the addition of carbon materials and fluxes. The main products generated in SAFs in ferroalloy production are molten metal and slag which accumulate during smelting and, therefore, must be removed from the furnace by performing an operation called tapping. During tapping, molten materials flow out through a tap-hole and into ladles, where the first ladle usually serves as a metal reservoir and subsequent ladles are used as slag reservoirs. Since the separation of metal and slag in the metal ladle occurs naturally due to their difference in density, slag tends to accumulate at the top of the metal ladle while metal settles to the bottom. Due to the turbulence of the tapping flow and interfacial interaction of metal and slag, metal droplets are formed in slag, forming a

so-called metal-slag emulsion.[1] After the first ladle is completely filled, slag begins to overflow to the slag ladles, entraining a large number of metal droplets. Metal entrained in slag is considered a loss, and this generally reduces the process efficiency,[2,3] mainly for the reason that further post-processing of slag with entrained metal droplets requires additional costs.

Interfacial phenomena are vital for ferroalloy production, as a better understanding of entrainment mechanisms can significantly help reduce ferroalloy losses with slag. The interfacial interaction between metal and slag and the stability of the interface between them are characterized by interfacial tension.[4] High interfacial tension promotes better separation, while the opposite is true for low interfacial tension. In metal-slag systems where surface-active elements such as sulfur, oxygen, selenium and tellurium are present, interfacial tension decreases as a result of higher mass transfer rates, leading to problems with the separation of metal and slag due to the formation of metal-slag emulsion.[5] In ferroalloys production, major elements which represent surface-active elements are sulfur and oxygen. For such systems, the thermodynamic equilibrium between ferroalloy and slag can be described by the reaction[6]:

$$[S] + (O^{2-}) \Leftrightarrow (S^{2-}) + [O], \qquad [1]$$
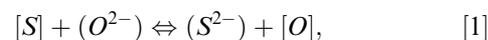
where $[S], [O]$ are sulfur and oxygen in alloy, $(S^{2-}), (O^{2-})$ are sulfur and oxygen in slag.

SERGEY BUBLIK, MERETE TANGSTAD, KRISTIAN ETIENNE EINARSRUD are with the Department of Materials Science and Engineering, Norwegian University of Science and Technology (NTNU), Trondheim, 7491, Norway. SARINA BAO is with SINTEF Industry, Trondheim, 7034, Norway. Contact e-mail: sergey.bublik@ntnu.no
Manuscript submitted January 22, 2021; accepted September 5, 2021.

Experimentally, the interfacial tension between two molten materials is typically determined by melting materials in a furnace equipped with an X-ray camera[7] or by applying the sessile drop technique with a digital camera.[8] After recording images of the interfacial interaction between two phases, interfacial tension is obtained by solving the Young–Laplace equation (Eq. [2]) numerically,

$$\Delta P = \gamma \left(\frac{1}{R_1} + \frac{1}{R_2} \right), \qquad [2]$$

where ΔP is the pressure difference at the interface, γ is interfacial tension, R_1 and R_2 are the principal radii of curvature,[9] which describes the relationship between interfacial tension and the shape of the interface. However, in most cases, the measurement of interfacial tension is extremely complicated due to high temperatures and complex composition of molten materials.

The present study is based on methodologies for the measurement of interfacial tension and apparent contact angles between ferroalloy and slag, which were developed and verified by the authors previously.[10,11] Interfacial interaction in synthetic FeMn-slag and SiMn-systems, both with and without sulfur addition to ferroalloy, has been investigated by combining analysis of images from a sessile drop furnace and

multiphase flow simulations in OpenFOAM v6,[12] and discussed together with the assessment of the sensitivity of the results by comparing different experiments.

II. EXPERIMENTAL

A. Material Preparation

Synthetic FeMn, SiMn and their corresponding slags have been prepared from pure powders for studying interfacial interactions in the sessile drop furnace. The composition of the synthetic materials has been chosen according to the composition of the industrial materials[2] as shown in Table I. The purity of chemicals used for material preparation is specified in Table II. The amount of each chemical required to produce corresponding synthetic materials has been calculated taking into account both the purity of chemicals and the composition of industrial materials and is presented in Table III.

The powders were mixed and melted separately in a graphite crucible in an induction furnace in Ar atmosphere at temperatures up to 1773 K for FeMn and 1873 K for SiMn. The holding time for preparation of FeMn and SiMn was 60 min, and for slags—5 min. After the melting, both ferroalloys and slags were ground in a ball mill and divided into batches of 50 g. Iron(II) sulfide

Table I. Chemical composition of industrial FeMn, SiMn and Slags[2]

Material	Chemical Composition (Wt Pct)								
	Mn	Fe	Si	C	MnO	CaO	MgO	SiO$_2$	Al$_2$O$_3$
FeMn	78	15	–	7	–	–	–	–	–
SiMn	68	12	18	2	–	–	–	–	–
FeMn Slag	–	–	–	–	38	23	6	23	10
SiMn Slag	–	–	–	–	11	23	6	43	17

Table II. Purity of Chemicals

Material	Purity (Pct)								
	Mn	Fe	Si	MnO	CaO	MgO	SiO$_2$	Al$_2$O$_3$	FeS
Chemicals	99.90	99.98	99.90	99.00	95.00	99.00	99.50	98.00	99.90

Table III. Weight of Pure Chemicals Used for Producing Synthetic FeMn, SiMn and Slags

Material	Weight of Pure Chemicals (g)								
	Mn	Fe	Si	MnO	CaO	MgO	SiO$_2$	Al$_2$O$_3$	Total
FeMn	209.89	40.33	—	—	—	—	—	—	250.22
SiMn	173.64	30.62	45.96	—	—	—	—	—	250.22
FeMn Slag	—	—	—	95.96	60.53	15.15	57.79	25.51	254.94
SiMn Slag	—	—	—	27.78	60.53	15.15	108.04	43.37	254.87

powder has been added to batches of FeMn and SiMn to provide 0.33, 0.66 and 1.00 wt pct of sulfur as shown in Table IV. Thereafter, both ferroalloys and slag were remelted at the same operational parameters in the induction furnace. Note that the carbon has not been added as a raw material for melting as it is contained in the graphite crucible, which allows ferroalloys to be saturated with the required amount of carbon—7 and 2 wt pct for FeMn and SiMn, respectively.

B. Experimental Setup

The sessile drop furnace, as sketched in Figure 1, has been applied for investigating the interfacial interaction between FeMn-slag and SiMn-slag. The sessile drop furnace was equipped with a pyrometer and a C-type thermocouple for measuring temperature, and with a digital video camera (Sony XCD-SX910CR, Sony Corporation, Millersville, MD) with a telecentric lens (Navitar 1-50993D) for recording images of the molten samples with the resolution of 1280×1024 pixels at one frame per second after reaching the melting point of ferroalloys and slags. Every 10 to 15 experiments, the thermocouple was calibrated by melting pure Fe in Ar and assessing its melting temperature from recorded images. The experiments were performed using graphite substrates or cups in Ar atmosphere (6 N grade) according to the experimental matrices as demonstrated in Tables V and VI. Additionally, the surface of the graphite substrates and cups was cleaned with a paper towel dipped in ethanol or acetone and then dried using compressed air.

Two experimental methods (Figure 2), were employed in this study:

– Method A (Figure 3(a)), allowing to measure apparent contact angles between metal and slag.

Table IV. Weight of Iron(II) Sulfide Added to FeMn and SiMn (in g)

Material	Corresponding to		
	0.33 wt pct S	0.66 wt pct S	1.00 wt pct S
FeS	0.45	0.90	1.37

– Method B (Figure 3(b)), allowing to determine both interfacial tension and apparent contact angle between metal and slag.

Initially, it was planned to apply only method B for studying interfacial interaction for both FeMn-slag and SiMn-slag systems, but subsequently it was found that SiMn has a poor wetting towards graphite, forming a SiMn droplet instead of a molten layer in the graphite cup as it is illustrated in Figure 4. Therefore, method A was adopted for the SiMn-slag system.

After the experiments, the ferroalloys and slags were cast in epoxy, sectioned in the centre of the slag droplet, re-cast into epoxy, polished and coated with carbon prior to analysis in EOL JXA-8500F Electron Probe Micro Analyzer (EPMA). The composition of the ferroalloy and slag phases were measured in several points and then average composition of each phase was calculated. Elemental mapping was performed for several samples to show sulfur distribution between metal and slag. Additionally, the chemical composition of ferroalloys and slags prior to experiments was determined by X-ray fluorescence (XRF) and the combustion infrared detection technique (combustion-IR). The ferroalloys were analyzed for Mn, Fe, Si, S and C, whereas slags were analyzed for MnO, CaO, MgO, SiO_2, Al_2O_3 and FeO.

In addition, the surface tension of FeMn, SiMn and slags was measured using the sessile drop furnace by melting ferroalloy or slag pieces on a graphite substrate. Surface tension for FeMn and FeMn slag was measured at temperature of 1723 K and at 1923 K for SiMn and SiMn slag.

C. Methodology for Measurement of Surface and Interfacial Tension

The methodology for determination of slag-metal interfacial tension is based on measurements of surface tension, followed by a comparison of geometrical features obtained from multiphase computational fluid dynamics (CFD) simulations using OpenFOAM[12] and experiments in the sessile drop furnace. The complete procedure is described in Reference 11, with a summary is given in the following for reference.

The elliptic solution of the Young–Laplace equation[14] has been applied for measurements of slag surface tension. Here, surface tension is expressed as:
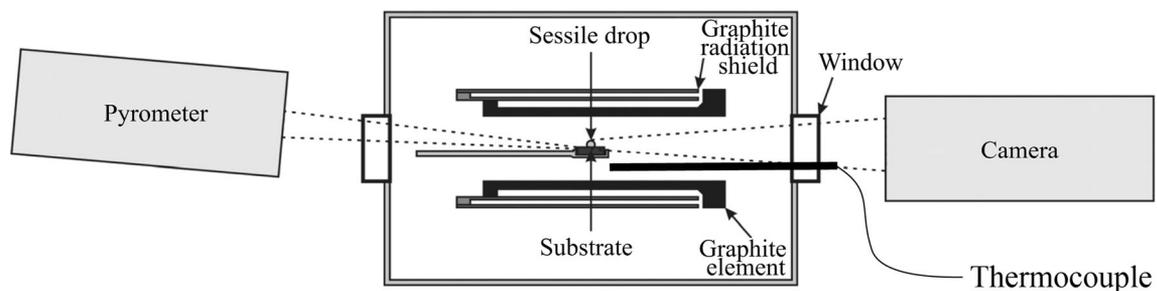

Fig. 1—Schematic overview of the sessile drop furnace. Modified from Ref. 13 under the terms of the Creative Commons CC BY license.

Table V. Experimental Matrix Used in Experiments for the FeMn-Slag System

Experiment	Calculated S Content (Wt Pct)	Maximum Temperature (K)	Holding Time at Maximum Temperature (Min)
1	0	1673	5
2	0.33	1673	5
3	0.66	1673	5
4	1.00	1673	5
5	0	1623	5
6	0	1723	5
7	0.66	1623	5
8	0.66	1723	5
9	0	1673	10
10	0	1673	15
11	0.66	1673	10
12	0.66	1673	15

Table VI. Experimental Matrix Used in Experiments for the SiMn-Slag System

Experiment	Calculated S Content (Wt Pct)	Maximum Temperature (K)	Holding Time at Maximum Temperature (Min)
13	0	1873	5
14	0.33	1873	5
15	0.66	1873	5
16	1.00	1873	5
17	0	1823	5
18	0	1923	5
19	0.66	1823	5
20	0.66	1923	5
21	0	1873	10
22	0	1873	15
23	0.66	1873	10
24	0.66	1873	15
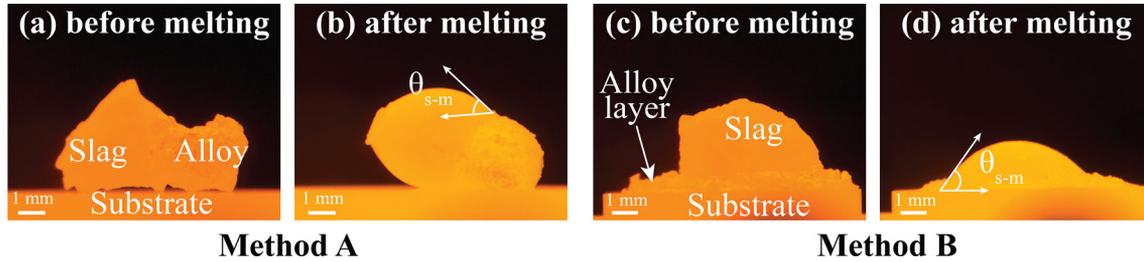
Fig. 2—Methods used for investigation of interfacial properties. In method A, ferroalloy and slag were placed on a graphite substrate. In method B, slag was placed on top of a ferroalloy layer in contact with a graphite cup. The interaction between slag and ferroalloy before melting for method A and B, respectively, is shown in images (a) and (c), while the interaction at the molten state is shown in images (b) and (d). Please note that the roughness on the surface of the droplets is related to the formation of solid carbon particles during the melting, which will be discussed further in Sect. III.B.

$$\gamma = \frac{a^2(\rho_{\text{slag}} - \rho_{\text{Ar}})g}{\frac{a^3}{b^3} + \frac{a}{b} - 2},$$ [3]

where g is the gravitational acceleration, ρ_{Ar} is the density of Ar (1.66 kg/m^3), ρ_{slag} is the density of slag in liquid state (3300 kg/m^3) for FeMn slag and 2700 kg/m^3 for SiMn slag.[15] Values of a and b are the length of the semi-minor and semi-major axis—respectively—found by fitting an ellipse to the slag contour. The elliptic solution results in a significant error in measurements in case if the droplet has a high wettability towards the substrate (contact angle < 90°) or if the surface of the droplet does not form a perfect circle or ellipse.

Surface tension of ferroalloys was measured by a plugin for ImageJ[16] based on low-bond axisymmetric drop shape analysis (LBADSA), which allows to fit the Young—Laplace equation to images and extract parameters of droplet's contour.[17] The main output from the plugin is the capillary constant c, which is used then to calculate the surface tension via the equation:
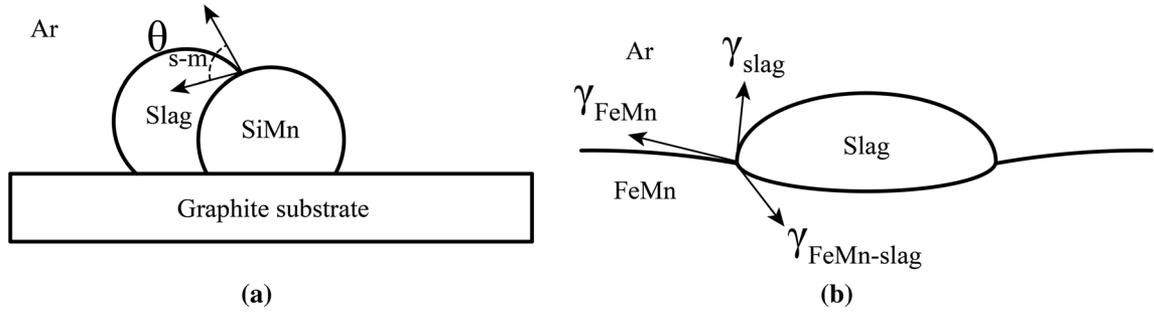
Fig. 3—Schematic demonstrating slag and ferroalloys at fully molten state in experiments. Image (*a*) shows slag and SiMn droplets in Ar atmosphere. θ_{s-m} is the contact angle between slag and SiMn. Image (*b*) shows the slag droplet floating on top of molten FeMn in Ar atmosphere. γ_{FeMn} is surface tension of FeMn, γ_{slag} is surface tension of slag, $\gamma_{FeMn-slag}$ is interfacial tension between FeMn and slag.


(a) before melting, 1475 K   **(b) after melting, 1671 K**
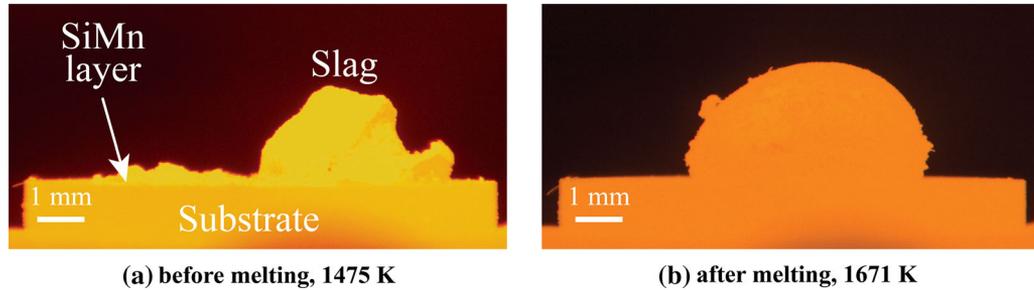
Fig. 4—Melting of SiMn layer and slag in the graphite cup in the sessile drop furnace. Image (*a*) shows the slag droplet and the SiMn layer before melting at 1475 K. Image (*b*) illustrates formation of a droplet rather than a layer.

$$c = \frac{(\rho_{metal} - \rho_{Ar})g}{\gamma}, \qquad [4]$$

where c is the capillary constant in m^{-2}, ρ_{metal} is the density of ferroalloys in liquid state $- 5612 \, kg/m^3$ for FeMn and $4449 \, kg/m^3$ for SiMn.[15]

The apparent contact angle between SiMn and slag has been measured every 30 to 60 seconds after 30 seconds of holding time—directly from images using the open source image processing software (ImageJ[18]).

The interfacial tension between FeMn and slag has been measured by method B approximately every 30 seconds after 2 minutes of holding time at minimum volume expansion of slag droplet to minimize the influence of volume fluctuations on the results. Method B, which is essentially based on comparing geometrical features obtained from simulations and experiments, consists of the following steps[11]:

(a) Conduct experiments in the sessile drop furnace with a single ferroalloy or slag droplet and determine surface tension of each material.
(b) Conduct experiments in the sessile drop furnace with a slag droplet placed on top of ferroalloy.
(c) Perform simulations in OpenFOAM for a defined range of interfacial tension using densities of ferroalloy and slag in the molten state, weight of the slag droplet and surface tensions determined at the first step. Calculate the non-visible height of the slag droplet (in pct) in the simulations.
(d) Measure the surface roughness correction coefficient (k_R) directly from experimental images as the average size of solid particles found at the FeMn-gas and slag-gas interface. In this study, k_R was up to 0.25 mm, depending on the surface roughness.
(e) Calculate the total volume of the slag droplet using slag density in the molten state and weight of the slag droplet measured before experiments:

$$V_{total} = \frac{m_{slag}}{\rho_{slag}}, \qquad [5]$$

where m_{slag} is weight of the slag droplet.
(f) Calculate the visible volume of the slag droplet (V_{vis}) in experiments assuming that the slag droplet forms a spherical cap both above and below the FeMn-gas interface and subtracting k_R from the visible height and the radius of the slag droplet:

$$V_{vis} = \frac{1}{6}\pi(h_{vis} - k_R)(3(a - k_R)^2 + (h_{vis} - k_R)^2), \qquad [6]$$

where h_{vis} is visible height of the slag droplet and a is radius of the slag droplet.

Table VII. Measured Chemical Composition (In Wt Pct) of FeMn and SiMn Alloys Before the Experiments in the Sessile Drop Furnace

Calculated S Content	Mn	Fe	Si	C	S	Total
FeMn Alloy						
0 wt pct	76.60	15.20	0.81	7.26	0.03	99.90
0.33 wt pct	75.50	15.70	0.57	7.22	0.04	99.03
0.66 wt pct	75.90	16.40	0.20	7.18	0.05	99.73
1.00 wt pct	74.50	17.10	0.20	7.18	0.11	99.09
SiMn Alloy						
0 wt pct	67.30	12.50	17.80	1.80	0.02	99.42
0.33 wt pct	67.40	12.90	16.30	2.00	0.25	98.85
0.66 wt pct	66.80	13.50	16.50	1.80	0.62	99.22
1.00 wt pct	66.80	14.00	16.50	1.70	0.90	99.90

Table VIII. Measured Chemical Composition (In Wt Pct) of FeMn and SiMn Slags Before the Experiments in the Sessile Drop Furnace

Material	MnO	CaO	MgO	SiO_2	Al_2O_3	FeO	Total
FeMn Slag	36.13	23.82	6.76	23.54	10.41	1.42	102.32
SiMn Slag	13.02	21.38	6.43	42.80	16.84	1.85	102.32

(g) Calculate the non-visible volume of the slag droplet ($V_{\text{non-vis}}$):

$$V_{\text{non-vis}} = V_{\text{total}} - V_{\text{vis}}, \qquad [7]$$

(h) Calculate the non-visible height of the slag droplet ($h_{\text{non-vis}}$) in the experiments:

$$V_{\text{non-vis}} = \frac{1}{6}\pi h_{\text{non-vis}}(3(a - k_R)^2 + h_{\text{non-vis}}^2), \qquad [8]$$

(i) Calculate the non-visible height of the slag droplet in pct:

$$h_{\text{non-vis}}(\text{pct}) = \frac{h_{\text{non-vis}}}{h_{\text{non-vis}} + h_{\text{vis}}} \cdot 100. \qquad [9]$$

(j) Compare experimental and simulation values to determine interfacial tension.

The 95 pct confidence interval for the sample mean was calculated based on the Student's t-distribution[19]:

$$CI = \overline{y} \pm t\frac{s}{\sqrt{n}}, \qquad [10]$$

where $\overline{y}$ is the sample mean, t is the critical value found from the confidence level and degrees of freedom of the sample, s is unknown sample standard deviation and n is the number of observations—from 6 to 31 in this study. Here, s is expressed as:

$$s = \sqrt{\frac{\sum_{i=1}^{n}(y_i - \overline{y})^2}{n - 1}}, \qquad [11]$$

where $y_i \{y_1, y_2, \ldots, y_n\}$ represents one measured value of the sample (i.e. single observation).

III. RESULTS AND DISCUSSION

A. Chemical Composition of Synthetic Ferroalloys and Slags

The chemical composition of ferroalloys before experiments was analyzed by XRF and combustion-IR and is summarized in Table VII, while the chemical composition of slags before experiments was analyzed by XRF and is given in Table VIII. Due to formation of FeMn dust and MnO_2 particles during combustion which then settle in the filter and lead to substantially lower sulfur values in the samples, sulfur content in FeMn could not reliably be determined by XRF and combustion-IR. Consequently, sulfur content in FeMn was estimated by EPMA from BSE images based on the surface area of the sulfide phase to the total area of the sample. The estimated sulfur content by EPMA is provided in Table IX.

Comparing the composition of the synthetic ferroalloys and slags with the composition of the industrial materials given in Table I, it is obvious that their compositions are close to a large extent, which indicates the correctness of the methodology used for the materials preparation in the current work.

B. Surface Tension of FeMn, SiMn and Corresponding Slags

The experimentally measured average values of surface tension by employing the aforementioned methodologies are presented in Figure 5. As it is expected for metals, FeMn and SiMn have higher values of surface tension – 1.50 and 1.20 N/m, respectively, while slags

have considerably lower surface tensions – 0.65 N/m for FeMn slag and 0.50 N/m for SiMn slag. Besides, sulfur addition to ferroalloys seems to have no significant effect on surface tension of FeMn and SiMn, which results in the same surface tension as corresponding alloys without sulfur addition. The LBADSA methodology, as it can be concluded from the confidence intervals, has a higher deviation in measurements of surface tension for FeMn, ±0.05 N/m. In contrast, the LBADSA for SiMn and the ellipsoidal solution of the Young-Laplace equation for slags result in smaller deviation, ±0.02 N/m. The difference can be explained by a rough surface of FeMn compared to other materials, as shown in Figure 6, which gives greater variation in measurements. The observed roughness of FeMn could be attributed to a higher C content, and hence more C can precipitate or dissolve during experiments with FeMn.

In all experiments with FeMn, solid carbon particles have been observed on top of FeMn layer as illustrated in Figure 7. Their formation may be caused by different temperatures during the materials preparation and the experiments. As it can be seen from Figure 8, the carbon saturation in FeMn is estimated to be 7.4 wt pct at melting temperature of 1773 K used in the induction furnace. However, at experimental temperatures of 1623 to 1723 K used in the sessile drop furnace, the carbon saturation decreases down to 7.0–7.3 wt pct and the rest

of carbon remains in solid state, which can consequently be observed on top of the FeMn layer in the experiments. A similar phenomenon of floating carbon particles on top of the FeMn melt was suggested by Hoel,[20] where it was discussed that excess carbon precipitates as graphite from the supersaturated melt as the temperature decreases. Figure 6(c) demonstrates that the amount of solid carbon precipitation on surface of the SiMn alloy is significantly lower compared to the FeMn alloy, since the melting of SiMn in the induction furnace at 1873 K and holding time of 60 minutes allowed to dissolve only ≈2 wt pct of carbon in the SiMn alloy and, as shown in Figure 9, this amount of carbon is completely dissolved in liquid SiMn at 1873 K.

It is worth mentioning that the evaporation of slag and metal droplets was not observed at the proposed temperatures (Figure 6) in the experiments for measurements of surface tension. The sample size over time only increased in all experiments due to thermal expansion. For instance, the volume change of the FeMn droplet was up to 10 pct higher after increasing temperature from the melting point (≈ 1533 K) to 1773 K, when surface tension was measured. The given sample size in this study was chosen to reduce the effect of solid carbon particles precipitation on the surface of FeMn, as decreasing the sample size is expected to introduce more uncertainty associated with the surface roughness. On the contrary, the variation in the droplet size (e.g. an

Table IX.   Sulfur Content in FeMn Estimated by EPMA

| Calculated S Content (Wt Pct)	MnS in the Total Area (Pct)	Chemical Composition of MnS Phase (Wt Pct)			S in FeMn (Wt Pct)
		Mn	S	Total	
0	0.08	62.62	38.27	100.90	0.03
0.33	0.80	63.33	38.87	102.20	0.31
0.66	1.48	63.36	38.70	102.50	0.57
1.00	2.40	63.21	38.62	101.83	0.93
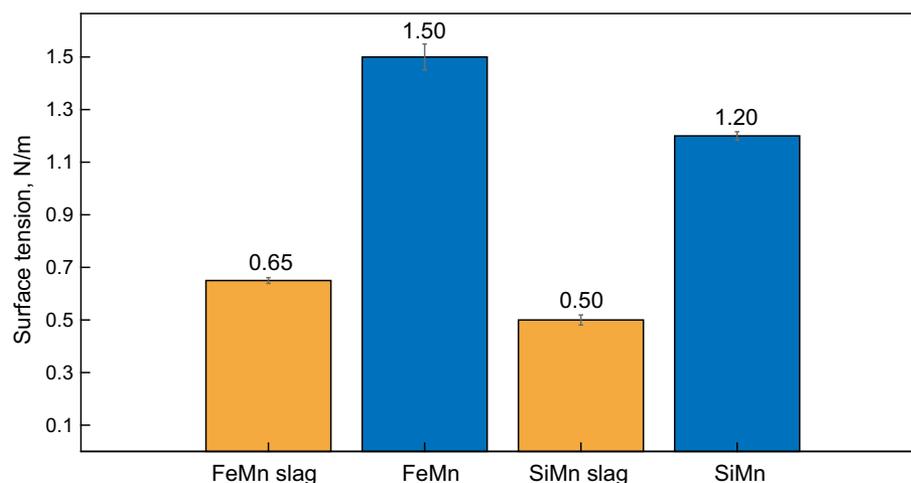
Fig. 5—Average values of surface tension of FeMn, SiMn and slags measured experimentally. Grey lines on top of bars represent the 95 pct confidence interval for the sample mean.

unreasonably big droplet) will also affect surface tension, as it can be inferred from Eq. [12], where the Eötvös number characterizes the balance between the gravitational force and the surface tension force,[21] and therefore the surface profile of a liquid droplet. However, no surface tension change was observed in the present study either using a droplet twice smaller or the given droplet size.

$$Eo = \frac{\Delta\rho g D^2}{\gamma} \left(\frac{\text{gravitational force}}{\text{surface tension force}} \right) \quad [12]$$

where Eo is the Eötvös number, $\Delta\rho$ is the density difference between two phases, D is the diameter of the droplet. High values of Eo specify that the droplet is strongly affected by the gravitational force, flattening the droplet, while low Eo values indicate that the droplet has the spherical shape.[22]

As it is has been reported by Lee et al.,[23] the surface tension of a pure Fe-system is 1.90 N/m, while Mn addition decreases the surface tension,[24] reaching surface tension of 1.00 N/m for a pure Mn-system without C addition. Assuming that there is no carbon present in FeMn used in the current work, which corresponds to 84 wt pct Mn and 16 wt pct Fe, the surface tension of FeMn of this composition according to Lee et al. is 1.10 N/m compared to 1.50 N/m measured experimentally for the high-carbon saturated FeMn alloy. There is no data published on surface tension of SiMn; therefore, as an analogue of the Fe-Mn

(a) FeMn at 1723 K

(b) FeMn slag at 1723 K

(c) SiMn at 1923 K
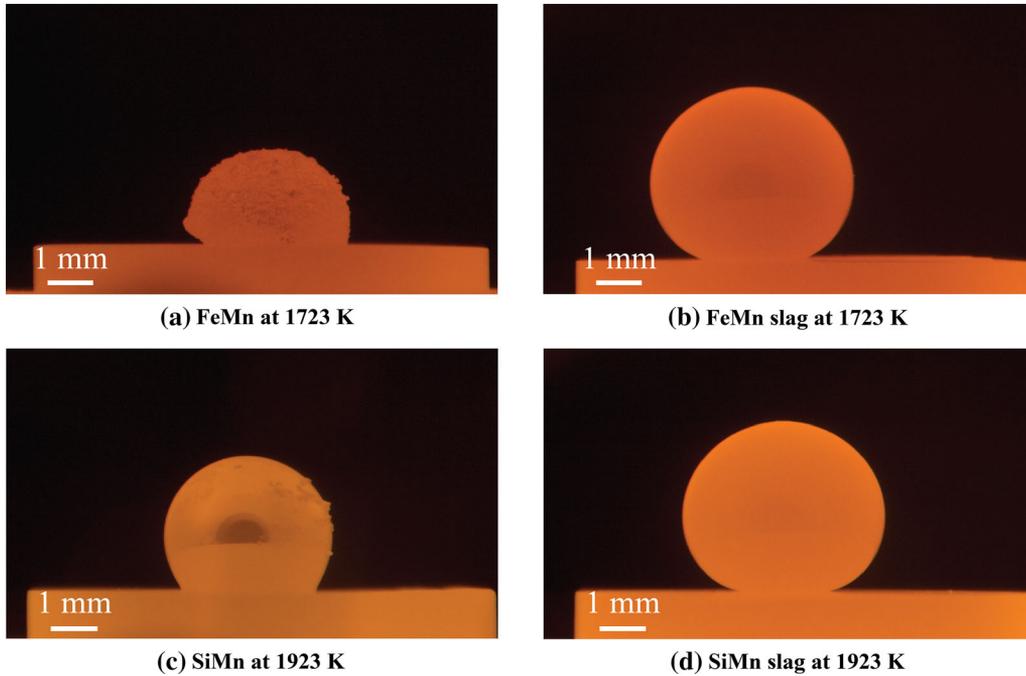
(d) SiMn slag at 1923 K

Fig. 6—Surface of FeMn, SiMn and slags during melting in the sessile drop furnace: (a) FeMn droplet at 1723 K, (b) FeMn slag droplet at 1723 K, (c) SiMn droplet at 1923 K, (d) SiMn slag droplet at 1923 K.

(a) FeMn and slag in experiments

(b) EPMA analysis
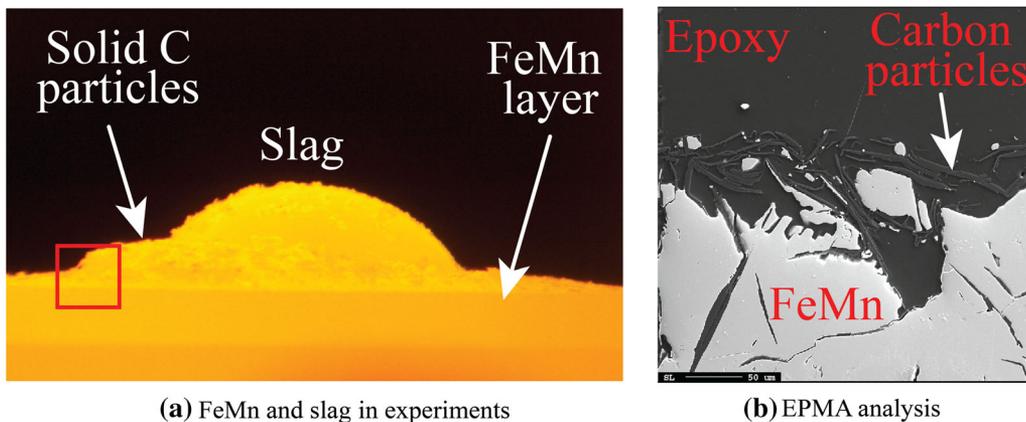
Fig. 7—(a) Slag droplet and solid carbon particles on top of FeMn layer during experiments. (b) EPMA image of the area indicated by the red box after experiments (Color figure online).
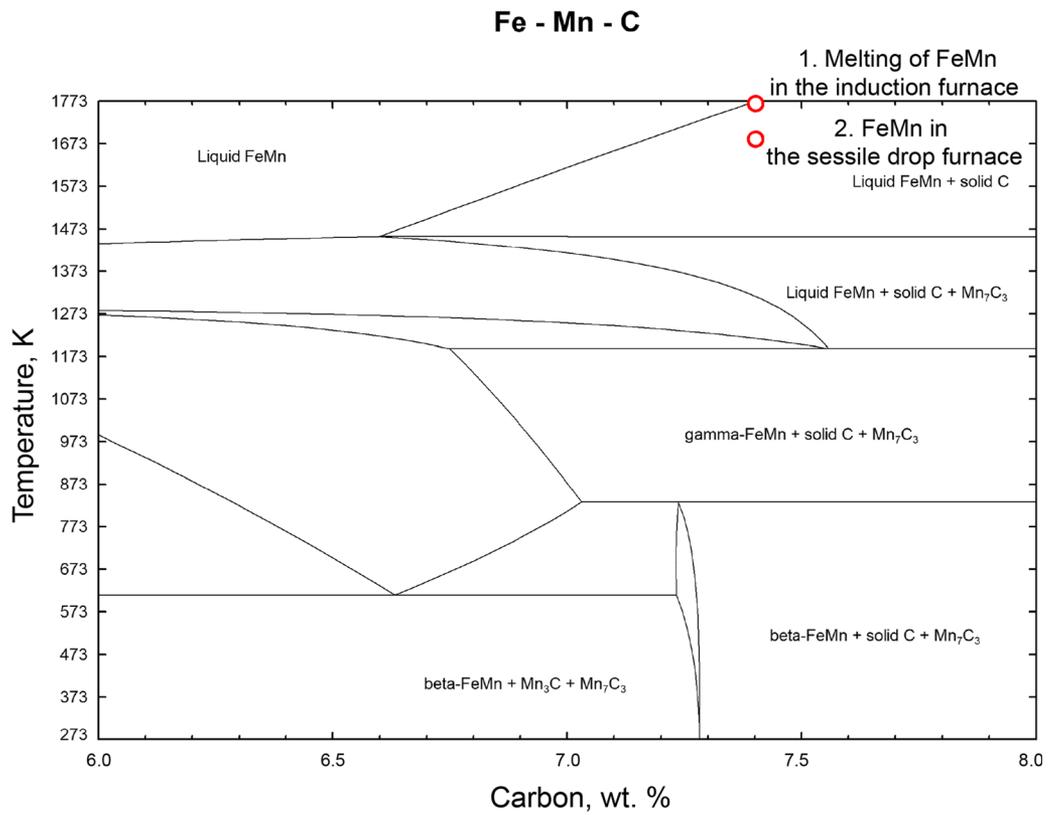
Fe - Mn - C

Fig. 8—Fe-Mn-C phase diagram calculated in FactSage 7.3 for constant Fe content of 15 wt pct.
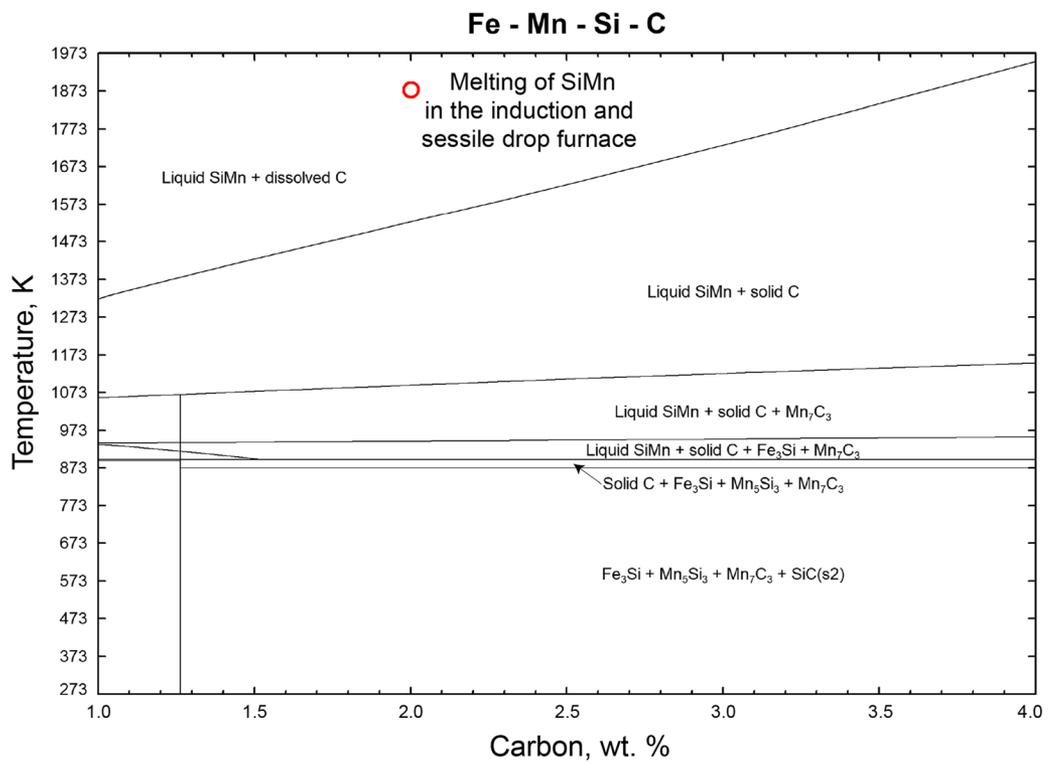
Fe - Mn - Si - C

Fig. 9—Fe-Mn-Si-C phase diagram calculated in FactSage 7.3 for constant Fe and Mn content of 12 and 68 wt pct, respectively.

system, surface tension can be alternatively described only for the Fe-Si system. The similar negative trend of Si on surface tension has been observed for a Fe-Si system,[25,26] where the addition of Si to pure Fe decreases surface tension from $\approx$ 1.80–1.90 to 0.70 N/m.

Lee and Morita[27] studied the surface tension of a Fe-C-S system, where they found that surface tension of a pure Fe gradually decreases with sulfur addition, which is caused by a high concentration of sulfur at the surface. In the present study, even though sulfur acts as a surface-active element, there is no interaction between sulfur in ferroalloys, the graphite substrate and Ar during melting in the sessile drop furnace. In addition, the applied LBADSA methodology is not able to determine small changes in surface tension due to the uneven surface of ferroalloy droplets. These two factors can explain constant surface tension with increasing sulfur content in ferroalloys from 0 to 1.00 wt pct.

Besides that, Lee and Morita[27] showed that C addition to pure Fe on alumina or aluminium nitride substrates increases surface tension. As it can be adopted for ferroalloys studied in this work, both FeMn and SiMn, being completely saturated with carbon after melting in the graphite crucible in the induction furnace, do not react with the graphite substrate, which results in a higher surface tension compared to non-carbon ferroalloy systems.

Depending on the composition, multicomponent slags generally have surface tension in the range from 0.30 to 0.70 N/m,[28,29] which corresponds to the ranges of surface tension found in the present study.

C. Effect of Sulfur Addition to Ferroalloy-Slag Systems

The effect of sulfur content in the SiMn alloy (S_{SiMn}) on the average apparent contact angle between SiMn and slag has been studied at constant maximum temperature of 1873 K and constant holding time of 5 minutes and is shown in Figure 10. The increase of S_{SiMn} from 0.02 to 0.90 wt pct decreases the average apparent contact angle from 37.8 to 29.6°. The largest change of $-$ 6.7° is observed between S_{SiMn} of 0.02 and 0.25 wt pct, while the change between S_{SiMn} of 0.25 and 0.62 wt pct, and between S_{SiMn} of 0.62 and 0.90 wt pct was only $-$ 1.1° and $-$ 0.4°.

The average interfacial tension between FeMn and slag changes depending upon sulfur content in the FeMn alloy (S_{FeMn}), as shown in Figure 11. The largest change of $-$ 0.30 N/m is noted when S_{FeMn} increases from 0.03 to 0.31 wt pct, which indicates that the equilibrium in the FeMn-slag-S system is reached in this range of S_{FeMn}. The further increase of S_{FeMn} to 0.93 wt pct decreases interfacial tension only slightly from 0.96 N/m to 0.88 N/m. However, the measurements for S_{FeMn} of 0.31 and 0.57 wt pct have a larger deviation described by confidence intervals of ± 0.09 and ± 0.05 N/m, respectively. As illustrated in Figure 12, these two experiments have significant fluctuations in surface area due to the gas evolution after 2 minutes of holding time at the maximum temperature, which most likely contributes to the variance observed in the experiments.

Sulfur, as a surface-active element, mainly concentrates at the surface or the interface and therefore the concentration of sulfur in the bulk does not play a significant role on the interfacial mass transfer, which reasonably means that the maximum concentration of sulfur at the interface is reached at S_{SiMn} of 0.25 wt pct and S_{FeMn} of 0.31 wt pct and the further increase of sulfur content in ferroalloys does not affect interfacial interaction in the FeMn-slag-S and SiMn-slag-S systems significantly. Suzuki et al.[30] have studied the effect of sulfur in a Fe-slag system on the dynamic change of apparent contact angle, where they found that sulfur absorbs at the Fe-slag interface and the apparent contact angle gradually decreases during reactions between metal and slag which is more pronounced with sulfur addition. Kim and Tangstad[31] studied the reduction kinetics of FeMn and SiMn slags in CO atmosphere at temperatures up to 1873 K. The authors
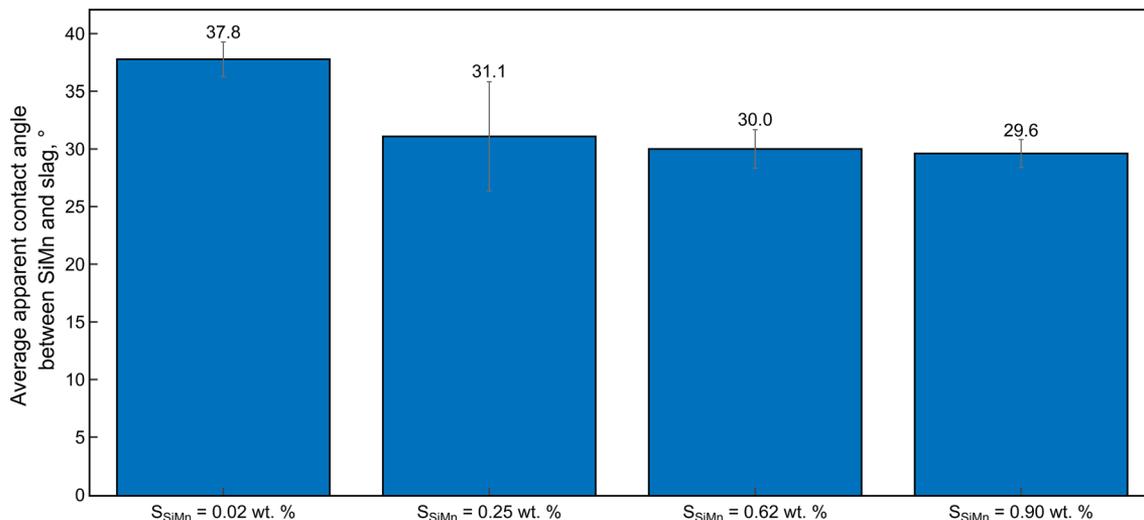

Fig. 10—Effect of sulfur content in SiMn on average apparent contact angle between SiMn and slag at temperature of 1873 K and holding time of 5 min. Grey lines on top of bars represent the 95 pct confidence interval for the sample mean.

reported that the initial sulfur content in slags changes the rate constant non-linearly, meaning that the rate constant reaches a maximum at a certain sulfur content in slag – 0.29 wt pct in their work. This may explain the surface area fluctuations in the experiments with S_{FeMn} from 0.31 to 0.57 wt pct in the given study, which are caused by higher reaction rates and thereby faster reactions between FeMn and slag.

Even though sulfur has not been added in experiment 13, sulfur is found to be evenly distributed between SiMn and slag as shown in Figure 13. This may indicate that sulfur was introduced to the SiMn-slag system from the powders or the graphite crucible during materials preparation or from the graphite substrate during the experiments. After increasing sulfur content in SiMn to 0.62 wt pct, the sulfur distribution shifts towards the slag phase and sulfur mainly concentrates in the bulk of

slag (Figure 14). The similar distribution of sulfur has been observed for the FeMn-slag-S system, in which sulfur is predominately found in the slag phase as illustrated in Figure 15. This was confirmed further by calculating the sulfur distribution in FactSage[32] (Figure 16), from which it is evident that sulfur tends to be distributed in slag, whether added to FeMn or SiMn.

D. Effect of Temperature

The effect of temperatures from 1823 to 1923 K on average apparent contact angle between SiMn and slag for S_{SiMn} of 0.02 and 0.62 wt pct at holding time of 5 minutes is shown in Figure 17. From this figure, one can notice that temperature has almost no effect on the apparent contact angle for S_{SiMn} of 0.02 wt pct, slightly decreasing it from 37.3° at 1823 K and 37.8° at 1873 K
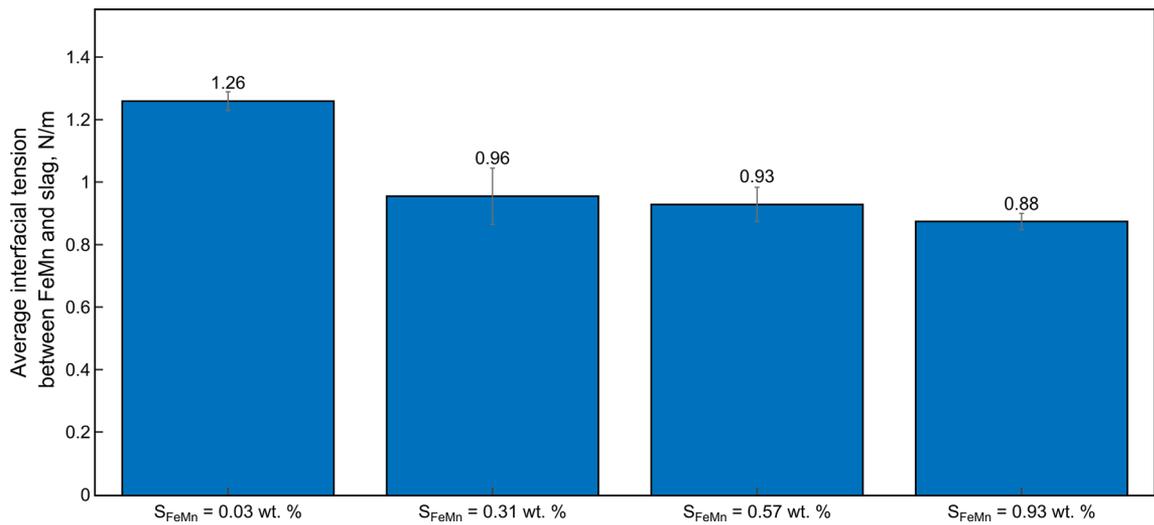
Fig. 11—Effect of sulfur content in FeMn on average interfacial tension between FeMn and slag at temperature of 1673 K and holding time of 5 min. Grey lines on top of bars represent the 95 pct confidence interval for the sample mean.
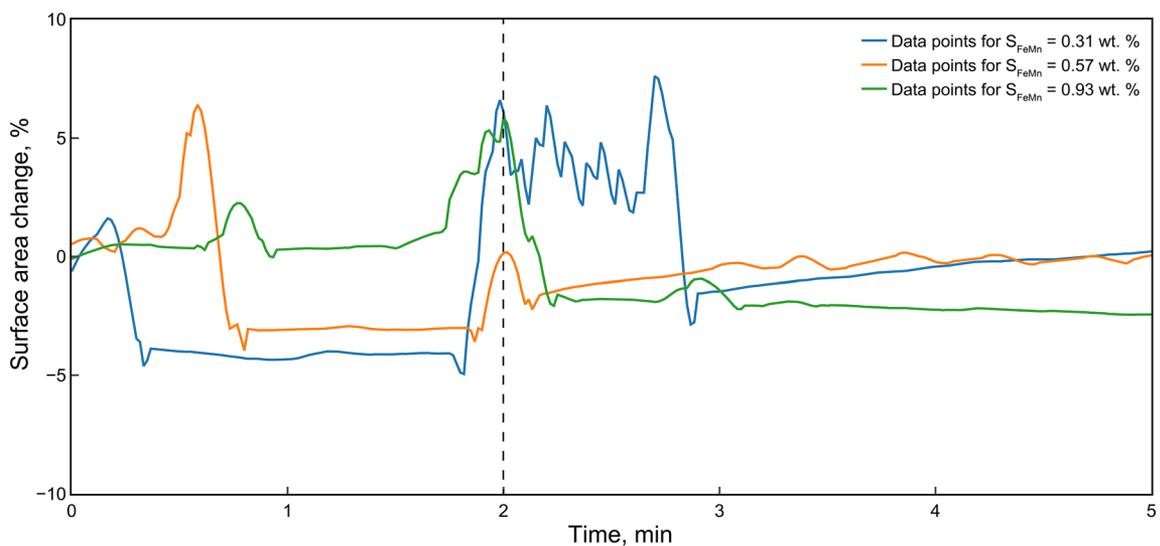
Fig. 12—Temporal change in visible surface area for experiments 2 to 4 during holding.

to 35.6° at 1923 K, $\Delta_{1823 \rightarrow 1923 K} = -1.7°$, $\Delta_{1873 \rightarrow 1923 K} = -2.2°$. However, for S_{SiMn} of 0.62 wt pct, the temperature influence is more evident, resulting in almost complete covering of SiMn by slag (Figure 18) and in a sharp decrease of apparent contact angle from 30.0 to 5.0° with increase of temperature from 1873 to 1923 K, $\Delta_{1873 \rightarrow 1923 K} = -25.0°$. Please note that the contact angle is challenging to determine from images as shown in Figure 18; however, the full dynamics observed in the recorded videos from the experiments allowed the contact angle to be determined based on the initial position of both droplets.

Similarly to the SiMn-slag-S system, temperature affects interfacial behaviour between FeMn and slag both with and without sulfur. As shown in Figure 19, average interfacial tension decreases considerably with temperature in the FeMn-slag-S system with 0.57 wt pct S, $\Delta_{1623 \rightarrow 1723 K} = -0.36$ N/m, compared to the system without sulfur addition, $\Delta_{1623 \rightarrow 1723 K} = -0.21$ N/m.

As it was found in other studies,[31,33] the mass transfer rate of sulfur tends to increase with temperature, resulting in more intensive reactions and therefore lower values of interfacial tension between metal and slag.

(a) BSE image
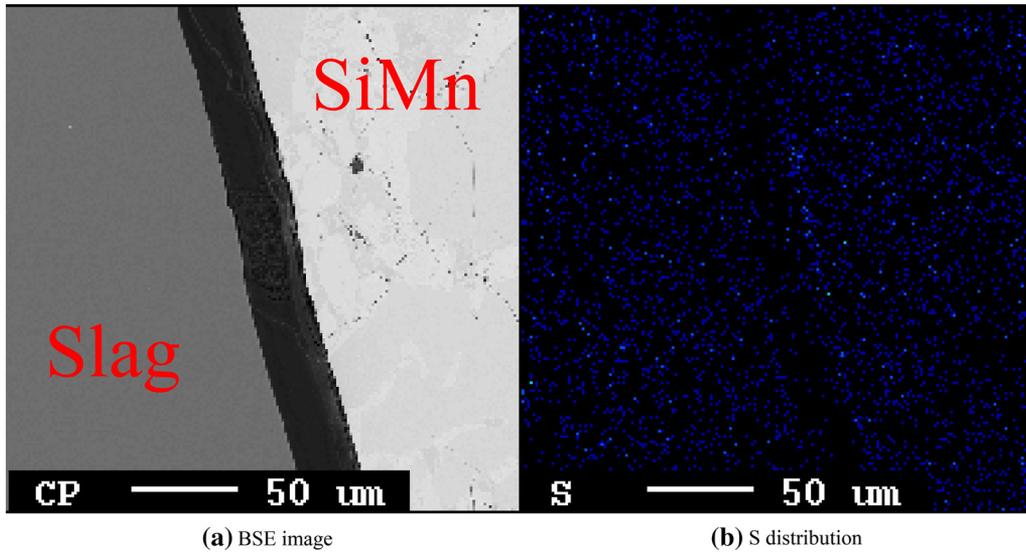
(b) S distribution

Fig. 13—EPMA results of the sample from experiment 13 (0.02 wt pct S_{SiMn}, 1873 K, 5 min holding time). (*a*) SiMn and slag on the BSE image, (*b*) EPMA elemental mapping showing sulfur distribution between SiMn and slag.

(a) BSE image
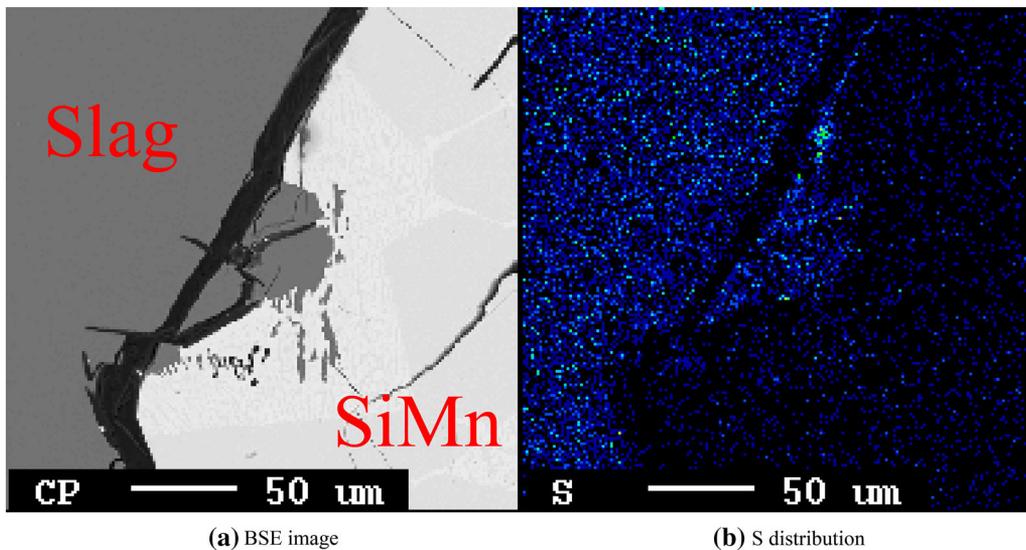
(b) S distribution

Fig. 14—EPMA results of the sample from experiment 15 (0.62 wt pct S_{SiMn}, 1873 K, 5 min holding time). (*a*) SiMn and slag on the BSE image, (*b*) EPMA elemental mapping showing sulfur distribution between SiMn and slag.

Due to the higher temperatures in experiments with the SiMn system, slag could be reduced by solid carbon, changing the initial slag composition and hence affecting the results. As found by EPMA and shown in Table X, slag composition changes after reaction with the SiMn alloy at different temperatures and, at lower temperatures, MnO reduces first.


(a) BSE image   **(b)** S distribution
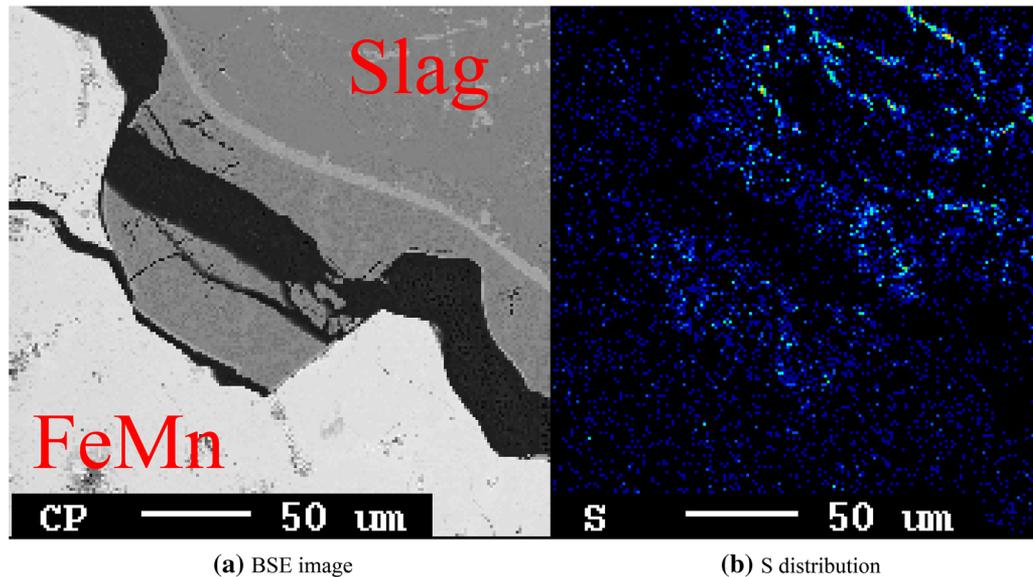
Fig. 15—EPMA results of the sample from experiment 2 (0.31 wt pct S_{FeMn}, 1673 K, 5 min holding time). (*a*) FeMn and slag on the BSE image, (*b*) EPMA elemental mapping showing sulfur distribution between FeMn and slag.
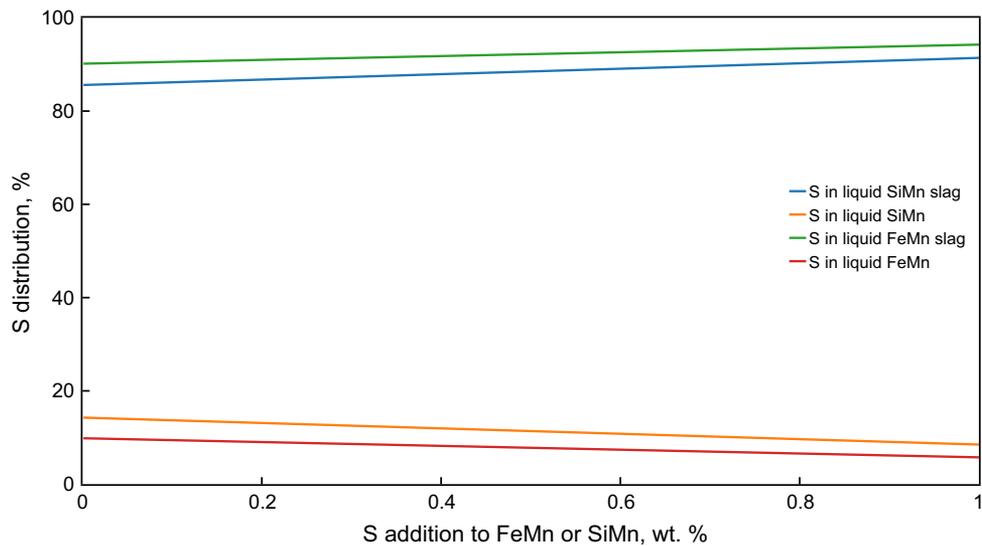
Fig. 16—Sulfur distribution between phases in the FeMn-slag-S-Ar and SiMn-slag-S-Ar systems at 1673 and 1873 K, respectively. Calculated using FactSage 7.3.

Table X. Slag Composition (In Wt Pct) After Reaction With the SiMn Alloy at Different Temperatures in the Sessile Drop Furnace

Temperature (K)	MnO	CaO	MgO	SiO$_2$	Al$_2$O$_3$	FeO	Total
1823	7.28	24.37	5.97	45.92	17.90	0.02	101.46
1873	6.38	25.14	6.17	44.71	18.65	0.01	101.06
1923	5.40	26.65	6.30	43.09	19.71	0.01	101.16
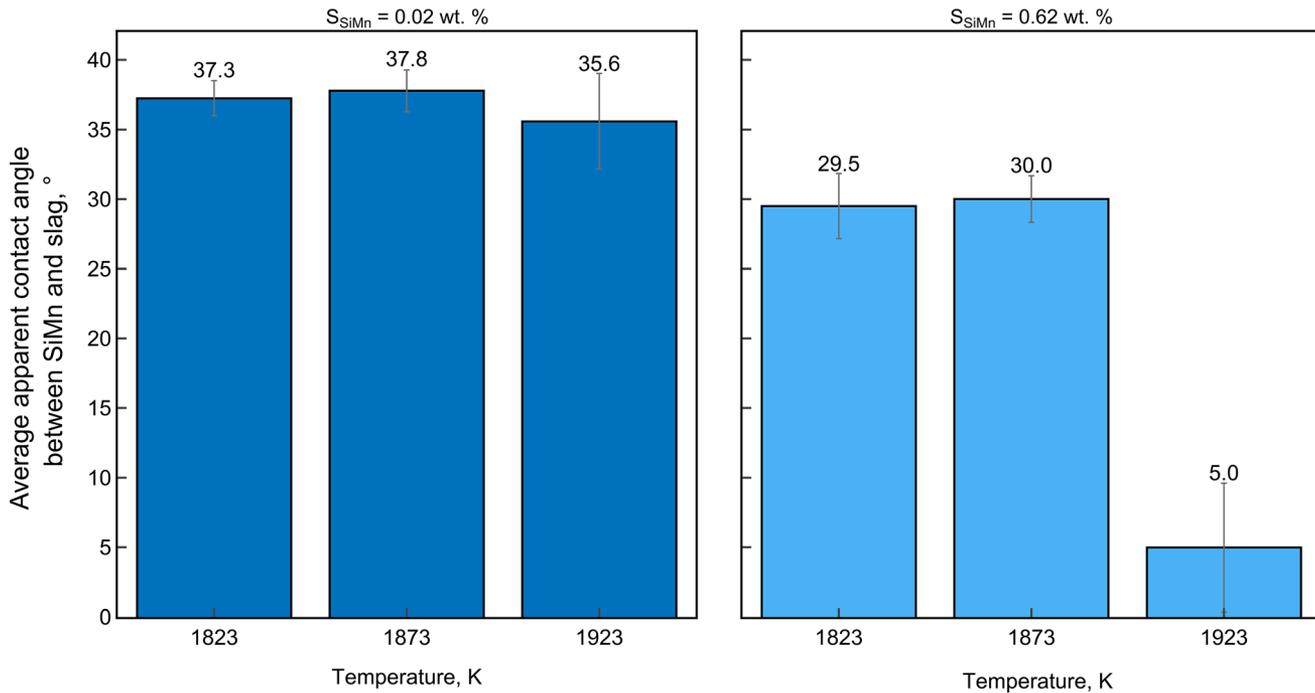
Fig. 17—Effect of temperature on average apparent contact angle between SiMn and slag at holding time of 5 min and different sulfur addition to SiMn. Grey lines on top of bars represent the 95 pct confidence interval for the sample mean.
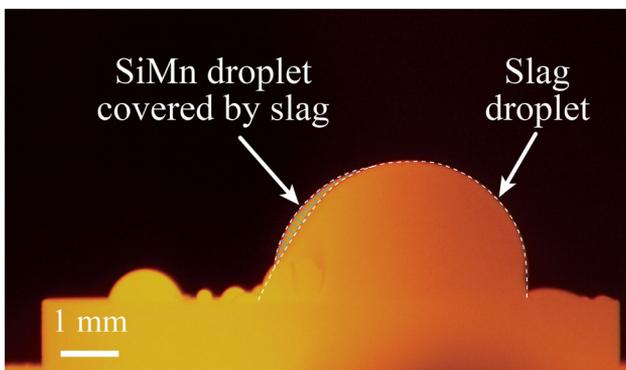

Fig. 18—SiMn and slag droplets at temperature of 1923 K. The hatched area represents the visible part of the SiMn droplet.

E. Effect of Holding Time

Figure 20 shows the influence of holding time of 5, 10 and 15 minutes on average apparent contact angle between SiMn and slag for S_{SiMn} of 0.02 and 0.62 wt pct at 1873 K. Similarly to temperature, holding time seems to have no effect on average apparent contact angle for S_{SiMn} of 0.02 wt pct, $\Delta_{5\rightarrow15\,min} = -1.0°$. Increasing holding time from 5 to 15 minutes for S_{SiMn} of 0.62 wt pct decreases average apparent contact angle between SiMn and slag from 30.0 to 20.1°. However, the largest change is observed with increasing holding time from 5 to 10 min, $\Delta_{5\rightarrow10\,min} = -9.4°$, while the change of holding time from 10 to 15 minutes has no significant effect on apparent contact angle, $\Delta_{10\rightarrow15\,min} = -0.5°$.

The effect of holding time on average interfacial tension between FeMn and slag is presented in Figure 21. For the FeMn system, varying holding time from 5 to 15 minutes seem to have no to little effect on interfacial tension, only insignificantly decreasing in experiments without sulfur and increasing when sulfur has been added to FeMn. Nevertheless, it should be noted that the confidence intervals for all holding experiments overlap, therefore, it is not possible to conclude about the negative or positive effect of holding time on interfacial tension.

Constant interfacial tension for the FeMn system and apparent contact angle for the SiMn system may indicate that the equilibrium in these systems has been reached and further holding does not affect the interfacial interaction. This also accords with previous observations,[30,34–36] where it was concluded that apparent contact angle between metal and slag dynamically changes with holding time, decreasing down to a certain minimum during the absorption of sulfur at the metal–slag interface. Subsequently, apparent contact angle stabilizes after increasing to a certain constant value, when sulfur is desorbed from the interface into the bulk of the molten metal and slag.

The sulfur distribution has been measured after the experiment with S_{FeMn} of 0.57 wt pct and holding time of 10 minutes (Figure 22). It can seen by comparison with Figure 15, that the distribution of sulfur to the slag phase does not change significantly as holding time increases from 5 to 10 min, further indicating that the equilibrium has already been achieved at holding time of 5 min.
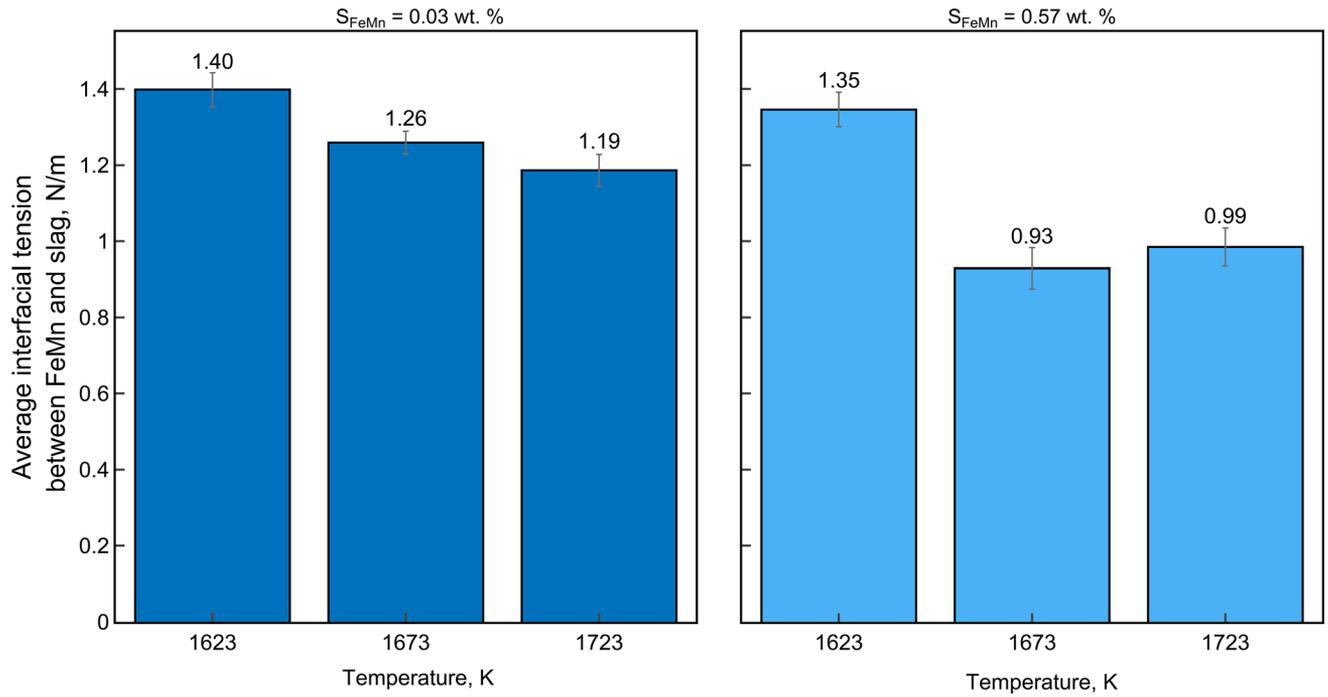
Fig. 19—Effect of temperature on average interfacial tension between FeMn and slag at holding time of 5 min and different sulfur addition to FeMn. Grey lines on top of bars represent the 95 pct confidence interval for the sample mean.
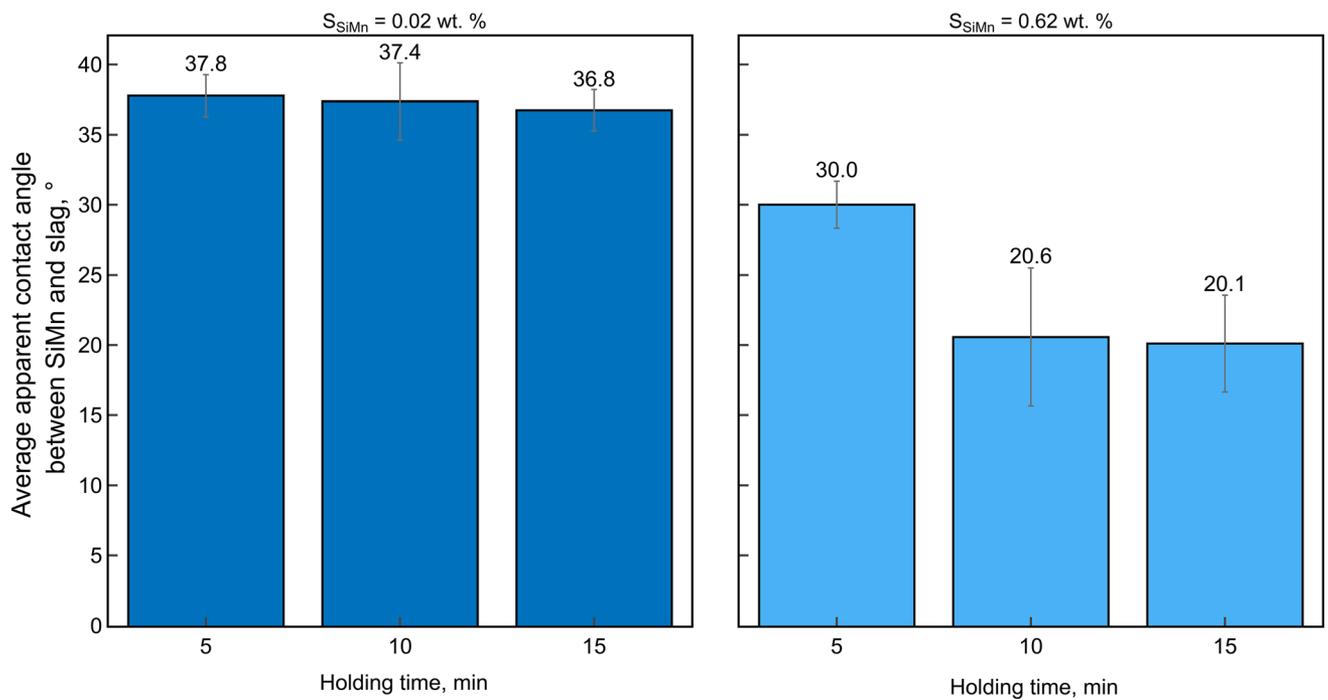

Fig. 20—Effect of holding time on average apparent contact angle between SiMn and slag at temperature of 1873 K and different sulfur addition to SiMn. Grey lines on top of bars represent the 95 pct confidence interval for the sample mean.

The data described statistically for experiments with the FeMn-slag-S and SiMn-slag-S systems is shown in Appendix A. Dynamic evolution towards the steady state for both systems is illustrated in Appendix B, where it is clear that there is a strong indication of reactions between slag and metal during the experiments, which partially explains uncertainties in the measured values.
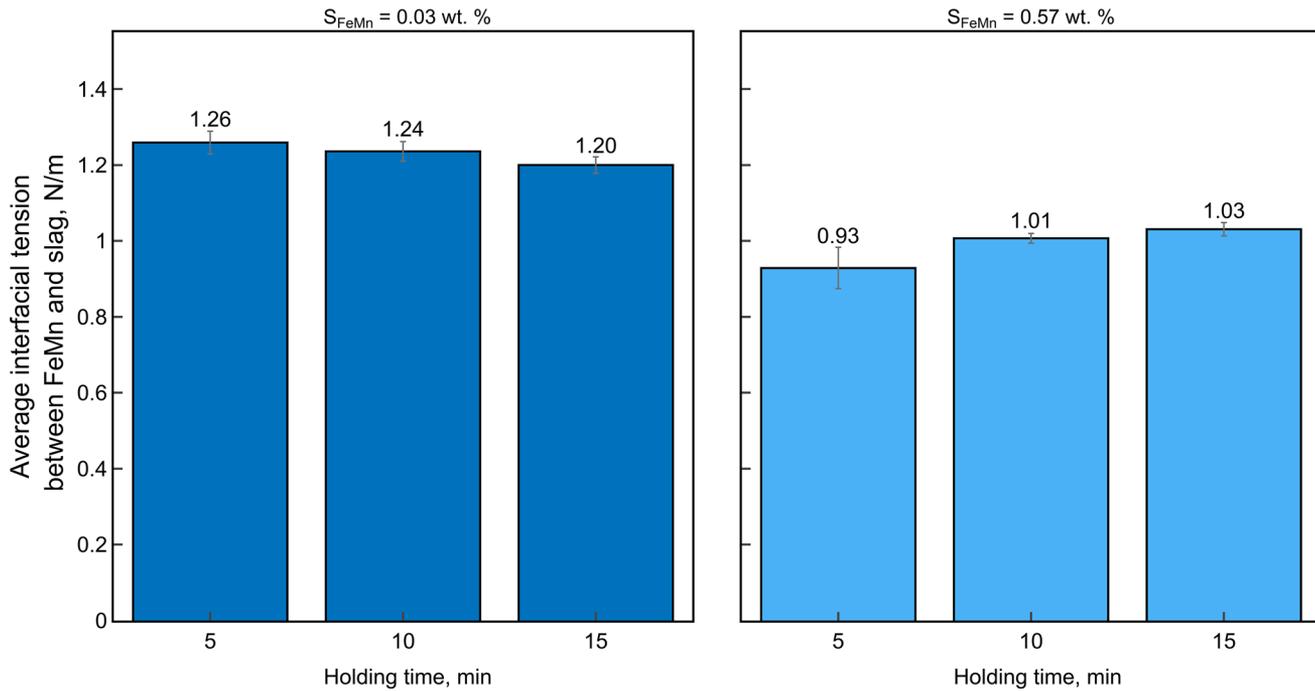
Fig. 21—Effect of holding time on average interfacial tension between FeMn and slag at temperature of 1673 K and different sulfur addition to FeMn. Grey lines on top of bars represent the 95 pct confidence interval for the sample mean.

(a) BSE image   (b) S distribution
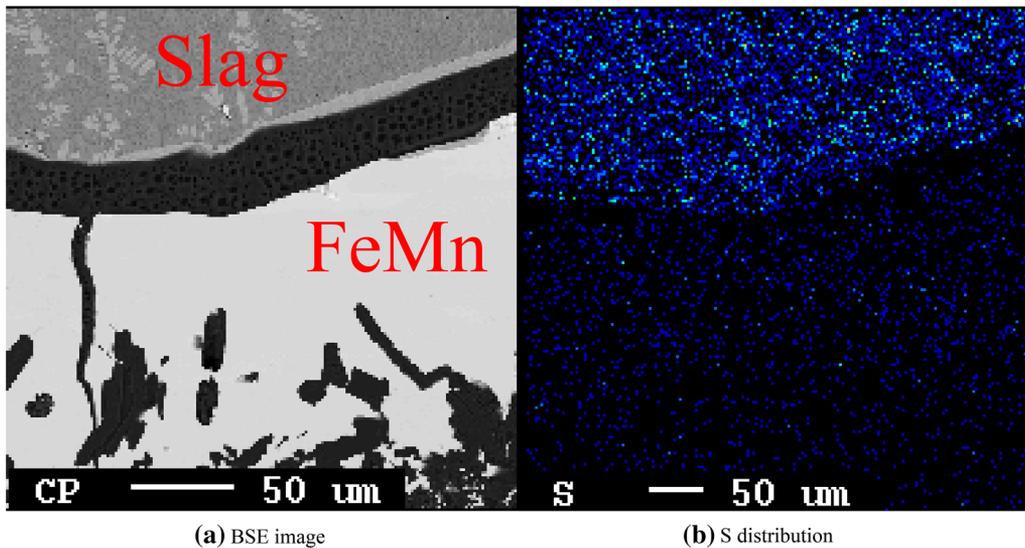
Fig. 22—EPMA results of the sample from experiment 11 (0.57 wt pct S_{FeMn}, 1673 K, 10 min holding time). (a) FeMn and slag on the BSE image, (b) EPMA elemental mapping showing sulfur distribution between FeMn and slag. Note that the images were taken from the same region at different magnifications.

IV. CONCLUSIONS

Sulfur plays a major role in the separation of metal and slag in ferroalloy production due to its ability to change the interfacial energy at the metal-slag interface, which leads to the formation of metal-slag emulsion and therefore additional metal losses with slag. In this study, the influence of sulfur added to FeMn or SiMn on the interfacial interaction between ferroalloy and slag has been investigated in a sessile drop furnace by applying different methodologies for FeMn and SiMn systems and comparing statistical data calculated from experimental results.

One of the more significant findings to emerge from this study is that there is a maximum of the extent to which sulfur can change interfacial tension and apparent contact angle between ferroalloy and slag—the maximum change was found at 0.25 wt pct sulfur in the SiMn alloy and 0.31 wt pct sulfur in the FeMn alloy. For all sulfur additions to ferroalloys, it is observed that sulfur

distributes mainly to slag after reaching equilibrium and the amount of sulfur remaining in the metal phase is less than 15 pct.

It has been also noted that the effect of temperature on interfacial tension and apparent contact angle is more noticeable in ferroalloy-slag systems with sulfur addition, which can be explained by a higher mass transfer rate and a larger interfacial area in such systems.

The holding time seems to have a limited effect on both interfacial tension and apparent contact angle. Despite small changes observed for both systems, these results must be interpreted with caution, since the confidence intervals in all holding time experiments overlap greatly. These small changes in interfacial properties may indicate that equilibrium in the SiMn-slag system and FeMn-slag system with and without sulfur is achieved before 5 minutes of holding time, while for the SiMn-slag-S system equilibrium is reached at 10 minutes of holding.

Solid carbon particles have been found on top of the FeMn layer and thereby the improvement of the materials preparation methodology might be necessary to reduce the uncertainty in measurements—for example, using crucibles made of other materials than graphite or chemical reagents of a higher purity. However, this might also introduce additional experimental difficulties in saturating the required amount of carbon, since in this case it has be added as a raw material. Besides, interfacial tension has not been measured for the SiMn system due to the fact that only graphite cups were used in the sessile drop furnace and a limited wettability of SiMn towards graphite. Therefore, experiments with cups made of different materials can be a further development of the current methodology.

APPENDIX A

See Appendix Tables XI and XII.

Table XI. Statistical Data for the Experiments With FeMn and Slag

| | Interfacial Tension Between FeMn and Slag (N/m) | | | |
Experiment	Mean	Standard Deviation	Standard Error	95 Pct Margin of Error
1	1.26	0.04	0.02	0.04
2	0.96	0.12	0.05	0.11
3	0.93	0.07	0.03	0.07
4	0.88	0.04	0.01	0.03
5	1.40	0.06	0.02	0.05
6	1.19	0.06	0.02	0.05
7	1.35	0.06	0.02	0.06
8	0.99	0.07	0.03	0.06
9	1.24	0.05	0.01	0.03
10	1.20	0.06	0.01	0.02
11	1.01	0.02	0.01	0.01
12	1.03	0.05	0.01	0.02

Table XII. Statistical Data for the Experiments With SiMn and Slag

| Experiment | Apparent Contact Angle Between SiMn and Slag (°) | | | |
	Mean	Standard Deviation	Standard Error	95 Pct Margin of Error
13	37.8	2.4	0.8	1.73
14	31.1	7.6	2.4	5.5
15	30.0	2.7	0.9	1.9
16	29.6	1.9	0.6	1.4
17	37.3	2.0	0.6	3.1
18	35.6	5.8	1.7	3.9
19	29.5	4.0	1.2	2.7
20	5.0	7.8	2.4	5.3
21	37.4	4.8	1.4	3.1
22	36.8	3.0	0.7	1.6
23	20.6	11.5	2.5	5.2
24	20.1	9.8	1.8	3.6

APPENDIX B

See Appendix Figs. 23, 24, 25, 26, 27, 28.
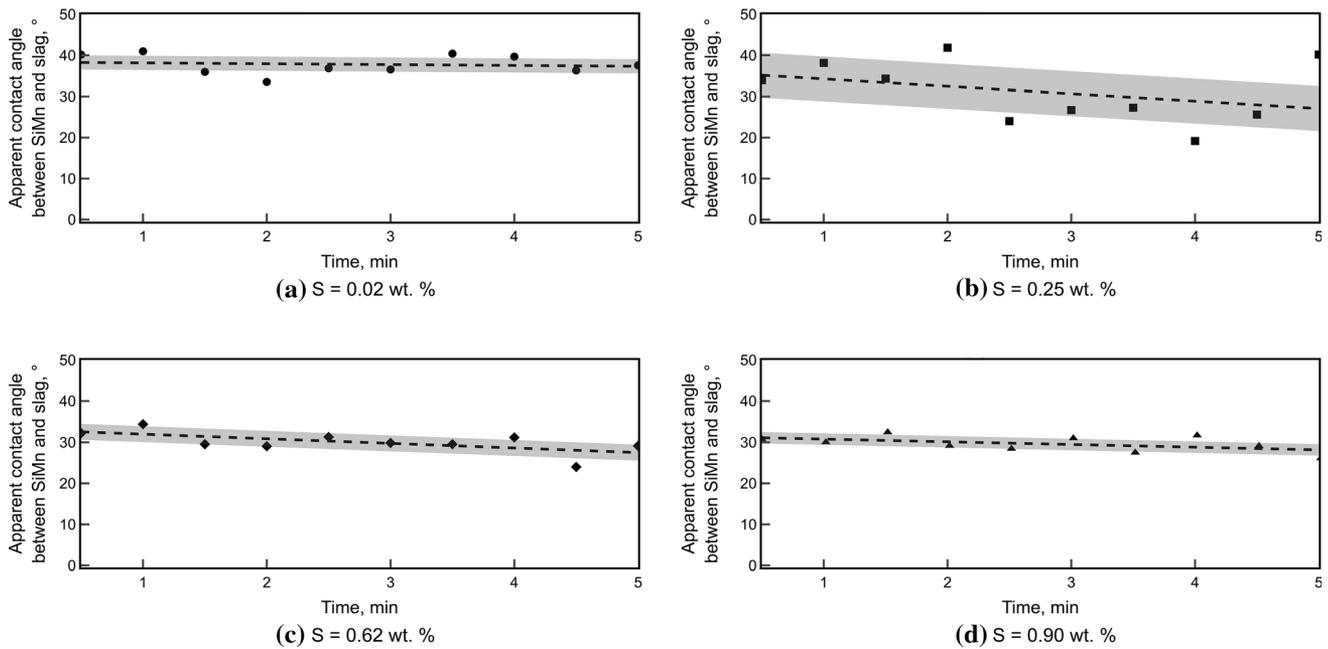
Fig. 23—Effect of sulfur on dynamic evolution of apparent contact angle between SiMn and slag at temperature of 1873 K and holding time of 5 min. The grey shaded area and the black dashed line represent the 95 pct confidence interval and the linear regression, respectively. Images (*a*) through (*d*) represent sulfur content in SiMn from 0.02 to 0.90 wt pct.

(a) S = 0.03 wt. %

(b) S = 0.31 wt. %

**(c)** S = 0.57 wt. %

(d) S = 0.93 wt. %
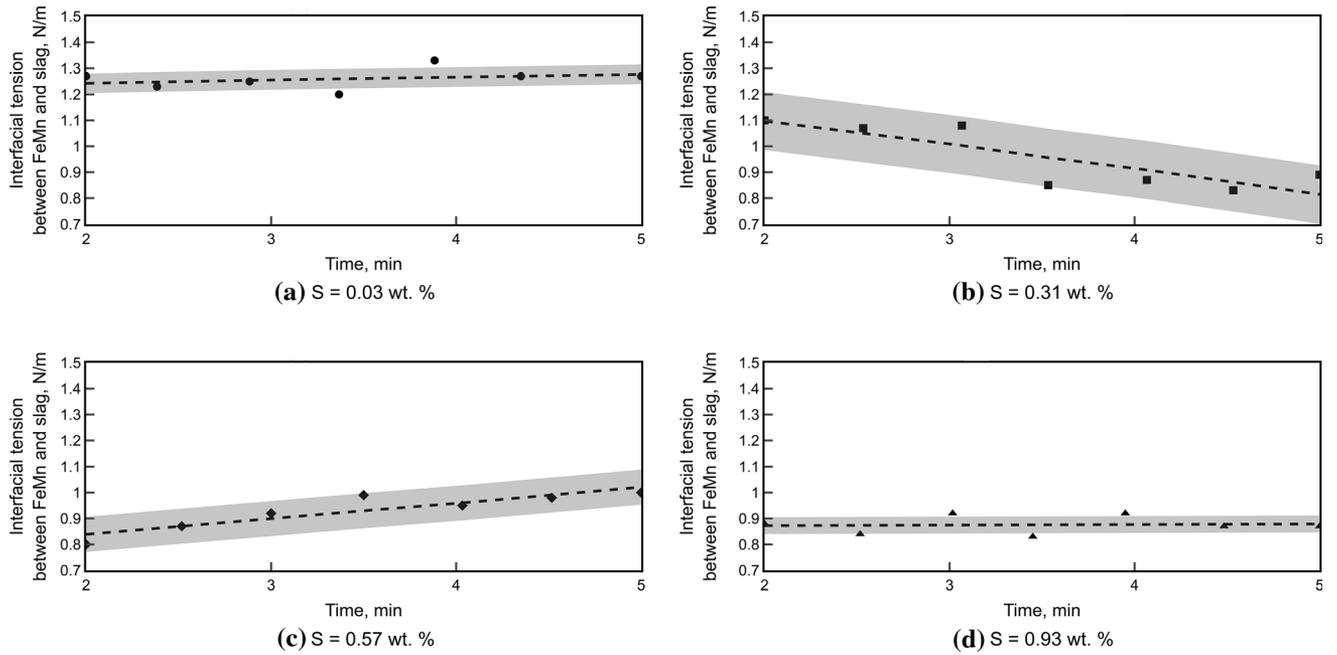
Fig. 24—Effect of sulfur on dynamic evolution of interfacial tension between FeMn and slag at temperature of 1673 K and holding time of 5 min. The grey shaded area and the black dashed line represent the 95 pct confidence interval and the linear regression, respectively. Images (*a*) through (*d*) represent sulfur content in FeMn from 0.03 to 0.93 wt pct.

(a) Temperature = 1823 K

**(b)** Temperature = 1873 K

(c) Temperature = 1923 K
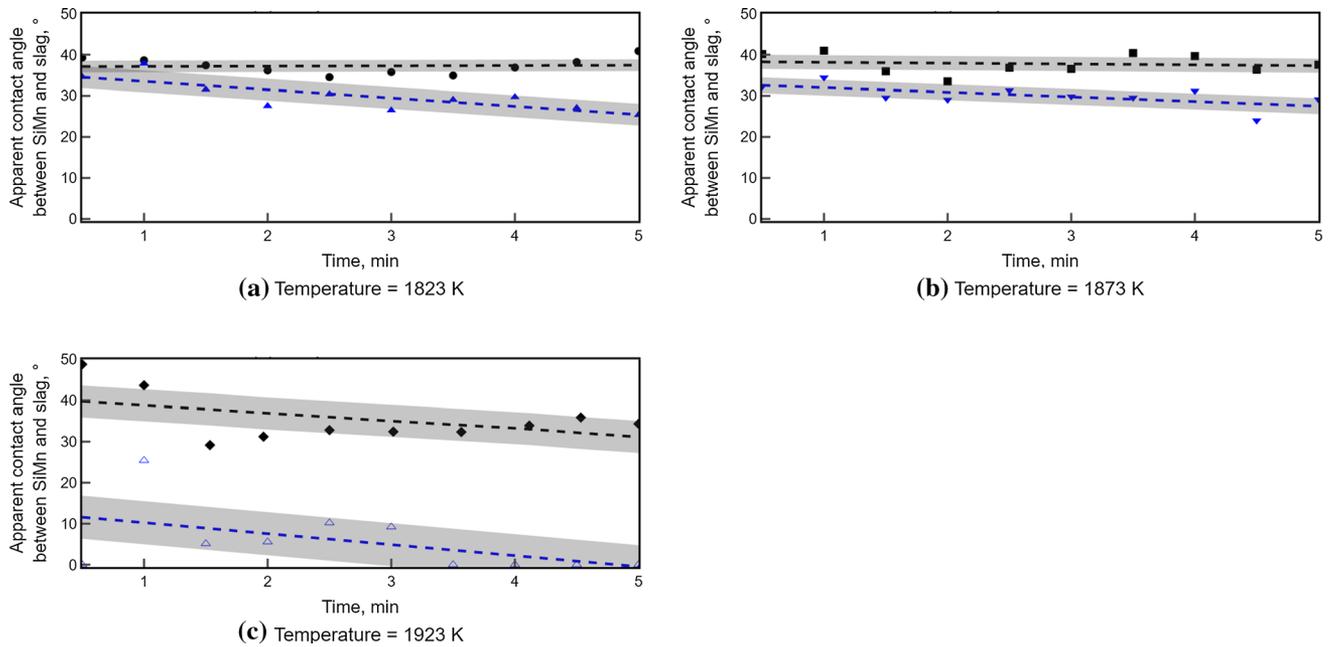
Fig. 25—Effect of temperature on dynamic evolution of apparent contact angle between SiMn and slag at holding time of 5 min. Black markers and lines refer to 0.02 wt pct S_{SiMn}, while blue markers and lines refer to 0.62 wt pct S_{SiMn}. The grey shaded area and dashed lines represent the 95 pct confidence interval and the linear regression, respectively. Images (*a*) through (*c*) represent temperature from 1823 to 1923 K.
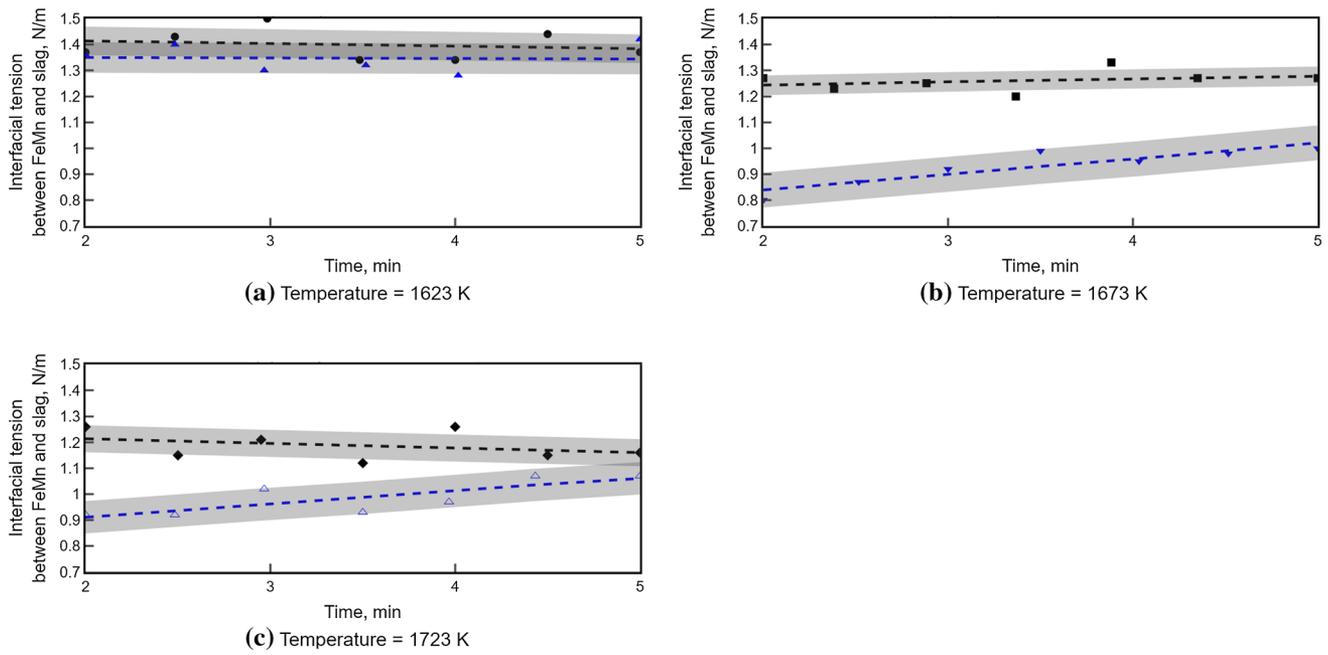
Fig. 26—Effect of temperature on dynamic evolution of interfacial tension between FeMn and slag at holding time of 5 min. Black markers and lines refer to 0.03 wt pct S_{FeMn}, while blue markers and lines refer to 0.62 wt pct S_{FeMn}. The grey shaded area and dashed lines represent the 95 pct confidence interval and the linear regression, respectively. Images (a) through (c) represent temperature from 1623 to 1723 K.
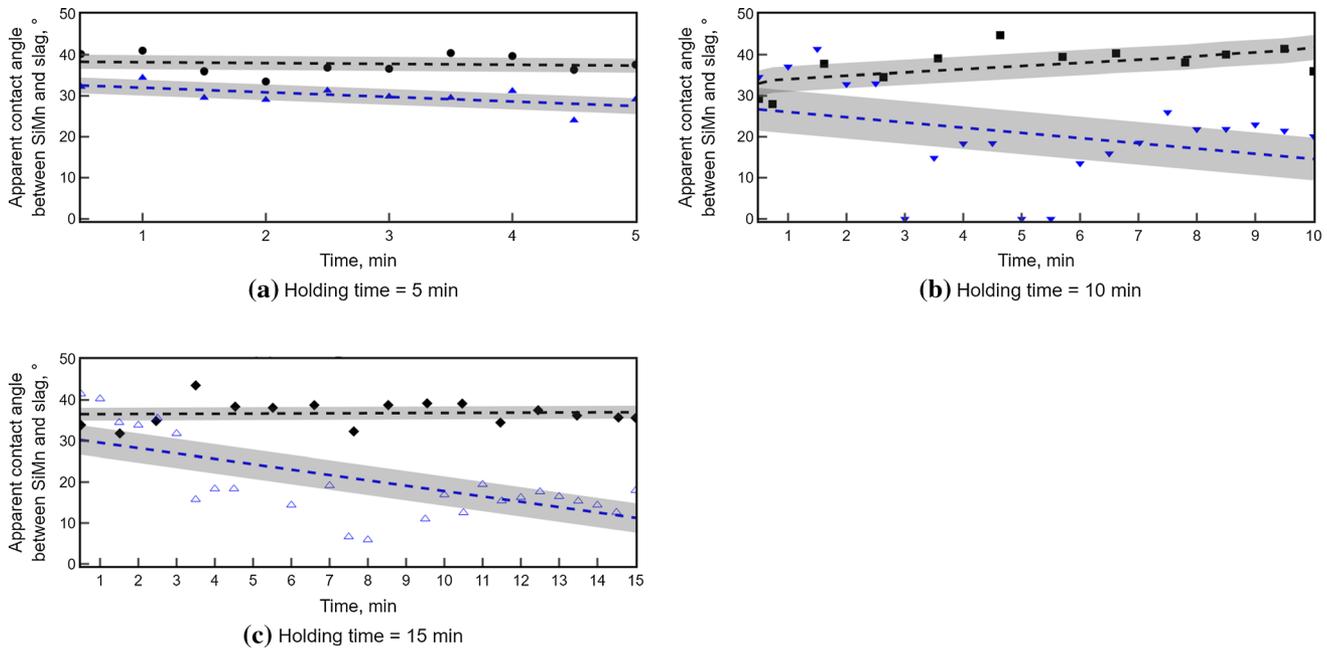

Fig. 27—Effect of holding time on dynamic evolution of apparent contact angle between SiMn and slag at temperature of 1873 K. Black markers and lines refer to 0.02 wt pct S_{SiMn}, while blue markers and lines refer to 0.57 wt pct S_{SiMn}. The grey shaded area and dashed lines represent the 95 pct confidence interval and the linear regression, respectively. Images (a) through (c) represent holding time from 5 to 15 min.
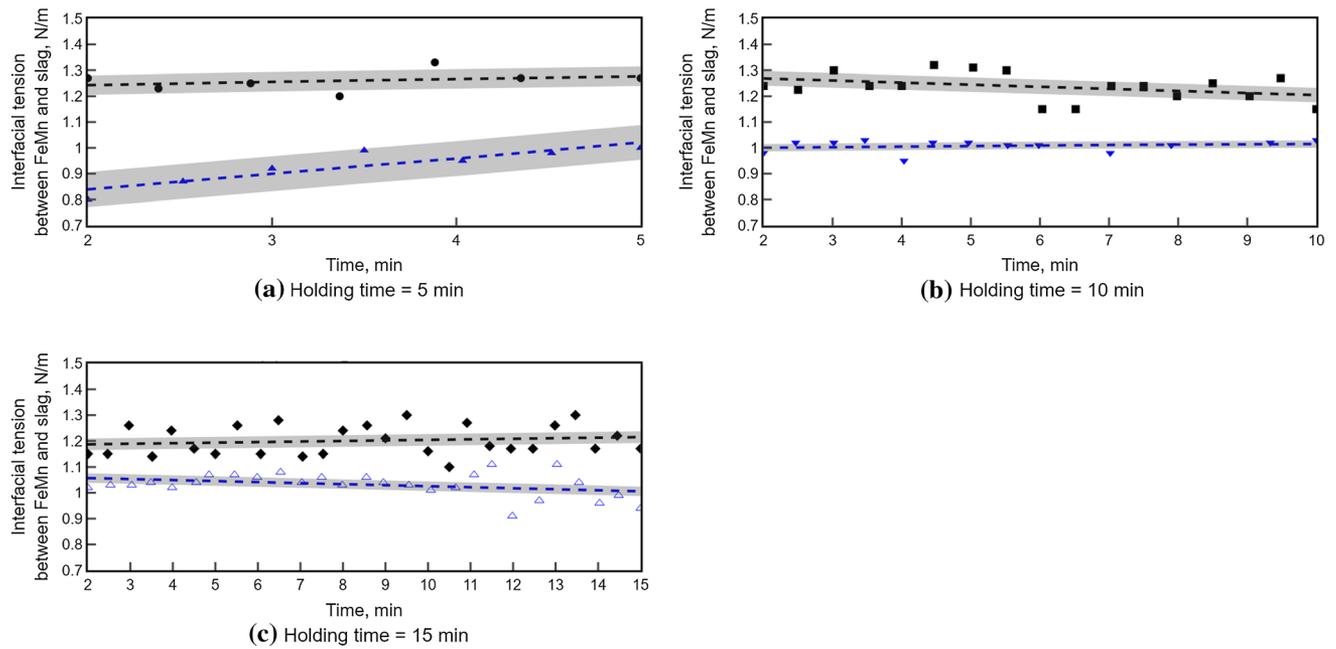
Fig. 28—Effect of holding time on dynamic evolution of interfacial tension between FeMn and slag at temperature of 1673 K. Black markers and lines refer to 0.03 wt pct S_{FeMn}, while blue markers and lines refer to 0.57 wt pct S_{FeMn}. The grey shaded area and dashed lines represent the 95 pct confidence interval and the linear regression, respectively. Images (*a*) through (*c*) represent holding time from 5 to 15 min.

REFERENCES

1. PR. Scheller, J. Lee, and T. Tanaka: *Treatise on Process Metallurgy: Chapter 1.8—Stability of Interface Between Liquid Steel and Molten Slag*, Elsevier, Boston, 2014, pp. 111–18.
2. M. Tangstad: *Handbook of Ferroalloys: Chapter 7—Manganese Ferroalloys Technology*, Butterworth-Heinemann, Oxford, 2013.
3. RH. Eric: *Treatise on Process Metallurgy: Chapter 1.10—Production of Ferroalloys*, Elsevier, Boston, 2014, pp. 477–32.
4. H. Ooi, T. Nozaki, and H. Yoshii: *Trans. Iron Steel Inst. Jpn.*, 1974, vol. 14, pp. 9–16.
5. AW. Cramb and I. Jimbo: *Steel Res.*, 1989, vol. 60, pp. 157–65.
6. H. Saridikmen, CS. Kucukkaragoz, and RH. Eric: *Sulphur Behaviour in Ferromanganese Smelting*, INFACON XI, New Delhi, 2007, pp. 311–20.
7. A. Jakobsson, D. Sichen, S. Seetharaman, and NN. Viswanathan: *Metall. Mater. Trans. B*, 2000, vol. 31, pp. 973–80.
8. E-J. Jung, W. Kim, I. Sohn, and D-J. Min: *J. Mater. Sci.*, 2010, vol. 45, pp. 2023–29.
9. E. Yakhshi-Tafti, R. Kumar, and HJ. Cho: *Int. J. Optomech.*, 2011, vol. 5, pp. 393–403.
10. S. Bublik, S. Bao, M. Tangstad, and K. E. Einarsrud: Slag-Metal Interactions in the FeMn Tapping Process: Interfacial Properties andWetting, Proceedings of the Liquid Metal Processing & Casting Conference 2019, Birmingham, UK, 2019, pp. 375–84.
11. S. Bublik and K. E. Einarsrud: Inverse Modelling of Interfacial Tension be436 n Ferroalloy and Slag Using OpenFOAM, 14th International Conference on CFD in Oil & Gas, Metallurgical and Process Industries, Trondheim, Nor438 SINTEF Academic Press, 2020, pp. 28–38.
12. HG. Weller, G. Tabor, H. Jasak, and C. Fureby: *Comput. Phys.*, 1998, vol. 12, pp. 620–31.
13. S. Bao, K. Tang, A. Kvithyld, M. Tangstad, and TA. Engh: *Metall. Mater. Trans. B*, 2011, vol. 42, pp. 1358–66.
14. E. Hernańdez-Baltazar and J. Gracia-Fadrique: *J. Colloid Interface Sci.*, 2005, vol. 287, pp. 213–16.
15. J. Muller, JH. Zietsman, and PC. Pistorius: *Metall. Mater. Trans. B*, 2015, vol. 46, pp. 2639–51.
16. AF. Stalder, T. Melchior, M. Müller, D. Sage, T. Blu, and M. Unser: *Colloids Surf. A*, 2010, vol. 364, pp. 72–81.
17. J. Lee, A. Kiyose, S. Nakatsuka, M. Nakamoto, and T. Tanaka: *ISIJ Int.*, 2004, vol. 44, pp. 1793–99.
18. CA. Schneider, WS. Rasband, and KW. Eliceiri: *Nat. Methods*, 2012, vol. 9, pp. 671–75.
19. DC. Montgomery: *Design and Analysis of Experiments*, 8th ed., Wiley, Hoboken, NJ, 2013.
20. E. G. Hoel: Phase Relations of Mn-Fe-Si-C Systems, INFACON 7, Trondheim, Norway, The Norwegian Ferroalloy Research Organization (FFF), 1995, pp. 601–10.
21. SK. Soni, PK. Kirar, P. Kolhe, and KC. Sahu: *Int. J. Multiph. Flow*, 2020, vol. 122, p. 103141.
22. J. Berthier: *Micro-Drops and Digital Microfluidics: Chapter 3–The Physics of Droplets*, 2nd ed., William Andrew Publishing, Burlington, 2013, pp. 75–160.
23. J. Lee, L. Thu Hoai, and M. Shin: *Metall. Mater. Trans. B*, 2011, vol. 42, pp. 546–49.
24. LT. Hoai and J. Lee: *J. Mater. Sci.*, 2012, vol. 47, pp. 8303–307.
25. BJ. Keene: *Int. Mater. Rev.*, 1988, vol. 33, pp. 1–37.
26. K. Mukai, T. Matsushita, KC. Mills, S. Seetharaman, and T. Furuzono: *Metall. Mater. Trans. B*, 2008, vol. 39, pp. 561–69.
27. J. Lee and K. Morita: *Steel Res.*, 2002, vol. 73, pp. 367–72.
28. J. Xin, N. Wang, M. Chen, and L. Gan: *ISIJ Int.*, 2019, vol. 59, pp. 759–67.
29. M. Hanao, T. Tanaka, M. Kawamoto, and K. Takatani: *ISIJ Int.*, 2007, vol. 47, pp. 935–39.
30. M. Suzuki, M. Nakamoto, T. Tanaka, Y. Tsukaguchi, K. Mishima, and M. Hanao: *ISIJ Int.*, 2020, vol. 60, pp. 2332–38.
31. PP. Kim and M. Tangstad: *Metall. Mater. Trans. B*, 2018, vol. 49, pp. 1185–96.
32. CW. Bale, E. Bélisle, P. Chartrand, SA. Decterov, G. Eriksson, AE. Gheribi, K. Hack, IH. Jung, YB. Kang, J. Melançon, AD. Pelton, S. Petersen, C. Robelin, J. Sangster, P. Spencer, and M-A. Van Ende: *CALPHAD: Comput. Coupling Phase Diagr. Thermochem.*, 2016, vol. 54, pp. 35–53.
33. Q. Wang, Y. Liu, F. Wang, Y. Cao, and G. Li: *Metals*, 2019, vol. 9, p. 751.

34. T. Tanaka, H. Goto, M. Nakamoto, M. Suzuki, M. Hanao, M. Zeze, H. Yamamura, and T. Yoshikawa: *ISIJ Int*., 2016, vol. 56, pp. 944–52.
35. P. Ni, T. Tanaka, M. Suzuki, M. Nakamoto, and PG. Jönsson: *ISIJ Int*., 2019, vol. 59, pp. 737–48.
36. P. Ni, T. Tanaka, M. Suzuki, M. Nakamoto, and PG. Jönsson: *ISIJ Int*., 2018, vol. 58, pp. 1979–88.